

Table 2 Clinical features of 20 male and 18 female patients with Danon disease

Characteristics	Male	Female
Subjects, n	20	18
Age, y, mean \pm SD	17 \pm 7 (n = 20)	38 \pm 12 (n = 14)
Age at onset, n		
Infantile	4	
Childhood	11	
Second decade	5	
Age at death, y, mean \pm SD	19 \pm 6 (n = 7)	40 \pm 7 (n = 6)
Cause of death, n (%)		
Cardiac failure	7/7 (100)	6/6 (100)
Myopathy, n (%)	18/20 (90)	6/18 (33)
Muscle weakness	16/20 (80)	6/18 (33)
Fatigability only	2/20 (10)	0/18 (0)
Cardiomyopathy, n (%)	20/20 (100)	18/18 (100)
Hypertrophic	16/19 (84)	2/7 (29)
Dilated	2/19 (11)	5/7 (71)
Mixed	1/19 (5)	
Mental retardation, n (%)	14/20 (70)	1/18 (6)
Elevated CK, n (%)	18/18 (100)	5/8 (63)
Serum CK (IU/L), mean \pm SD	1574 \pm 790 (n = 18)	
Serum AST (IU/L), mean \pm SD	382 \pm 234 (n = 12)	
Serum ALT (IU/L), mean \pm SD	344 \pm 199 (n = 11)	
Serum LDH (IU/L), mean \pm SD	1874 \pm 935 (n = 11)	
Serum aldolase (IU/L), mean \pm SD	17.4 \pm 8.0 (n = 9)	
Abnormal EKG, n (%)	17/17 (100)	10/10 (100)
Age at abnormal EKG, y, mean \pm SD	13 \pm 5 (n = 10)	
Abnormal echocardiogram, n (%)	19/19 (100)	3/3 (100)
Pacemaker, n (%)	6/20 (30)	3/18 (17)
Heart transplantation, n (%)	1/20 (5)	2/18 (11)
Myogenic EMG, n (%)	10/10 (100)	
Hepatomegaly, n (%)	5/14 (36)	
Splenomegaly, n (%)	1/13 (8)	
Foot deformity, n (%)	3/8 (38)	
Delayed milestone, n (%)	3/8 (38)	
Abnormal EEG, n (%)	2/7 (29)	
Manifesting mother, n (%)	14/20 (70)	6/18 (33)

CK = creatine kinase; AST = aspartate transaminase; ALT = alanine aminotransferase; LDH = lactate dehydrogenase; EMG = electromyography.

gression of the disease. For example, two male patients were first identified when isolated increases in serum creatine kinase were noted, and two others because they had abnormal EKG findings preceding cardiac symptoms. Only one male patient developed dyspnea in the infantile period; most commonly onset is of childhood onset. All patients were born through normal pregnancy and delivery. Delayed milestones with mild mental retardation were ob-

served in three male patients. Five male patients ran slower than their peers during childhood. The mean age at death was 19 years, with a range of 12 to 29 years; all died of cardiac failure or sudden cardiac arrest. No male patients survived beyond age 29 years except for a 34-year-old man in Family 1. He had mild cardiomyopathy but reported no cardiac symptoms.

All 20 male patients had cardiomyopathy. Most had hypertrophic cardiomyopathy, but two had dilated cardiomyopathy, and one had mixed features of hypertrophic and dilated cardiomyopathy. Permanent pacemakers were inserted in six male patients (30%). Heart transplantation was performed in one male patient (5%).

Myopathy was usually mild and was observed in 17 of 20 male patients (85%). The main symptoms were mild proximal limb and neck muscle weakness. All male patients remained ambulatory. Two male patients without weakness had only premature fatigability without fixed weakness. When present, muscle atrophy was mild. Only three male patients had obvious muscle wasting.

Mild mental retardation was observed in 14 male patients (70%). IQ was reduced to a range of 60 to 91 in five male patients in whom formal cognitive tests were performed.

On physical examination, hepatomegaly was observed in five of 14 male patients (36%) and splenomegaly in one of 13 male patients (8%). Foot deformities, such as pes cavus, was seen in three of eight male patients (38%).

Laboratory tests showed that serum creatine kinase and aldolase were increased five- to 10-fold above upper limits of normal. Creative kinase values ranged from 339 to 3,128, with an average of 1,574 \pm 790 IU/L (normal range: <220). In addition, serum aspartate transaminase, alanine aminotransferase, and lactate dehydrogenase levels were also increased (see table 2). On biochemical analyses, acid α -1,4-glucosidase activity was normal in most male patients but was increased in some.

EKG findings were abnormal in all male patients tested (n = 17, 100%). The most frequent pathologic finding was Wolff-Parkinson-White (WPW) syndrome (six male patients) with a short PQ interval, a prolonged QRS complex, and a delta wave. Male patients with hypertrophic cardiomyopathy showed abnormally high voltage in precordial leads. In addition, giant negative T wave, third-degree atrioventricular block, atrial flutter, bradycardia, abnormal Q wave, and complete left bundle branch block were also observed. The mean age at which abnormal EKG findings were first noticed was 13 \pm 5 years (n = 10). EKG also showed abnormalities in all male patients studied (n = 19); most had concentric hypertrophic cardiomyopathy with impaired left ventricular function. Seven male patients had abnormally thick interventricular septum and posterior walls. Electromyography showed small-amplitude short-duration motor unit potentials in all 10 male patients tested. In addition, fibrillation and positive sharp waves were present in three male patients, myotonic potentials at rest were noted in three individuals, and all three forms of abnormal discharges were noted in one. Nerve conduction studies were normal in all five male patients tested. Electroencephalography showed mild abnormalities in two of seven male patients; one had moderate bitemporal slowing and the other had slow α wave pattern with emergence of diffuse θ waves during sleep.

Table 3 Immunohistochemical and histochemical characteristics of skeletal muscle in Danon disease

Characteristic	Expression	Location
NSE	+	Vacuolar membrane
AchE	+	Vacuolar membrane
Acid phosphatase	+	Vacuolar material
Dystrophin	+	Vacuolar membrane and sarcolemma
Laminin	+	Vacuolar membrane and sarcolemma
Sarcoglycan	+	Vacuolar membrane and sarcolemma
LAMP-2	-	

NSE = nonspecific esterase; AchE = acetylcholinesterase.

Fourteen of the 20 mothers were symptomatic (70%). Four of the five asymptomatic mothers (80%) had single affected sons. *LAMP-2* gene sequences were normal in blood DNA of two asymptomatic mothers. The clinical features of 18 affected women are summarized in table 2.

It is difficult to define the age at onset in affected women because of the insidious nature of the disease. In the present study, the age at onset in the affected women was 38 ± 12 years (range, 12 to 53 years). Six women died (average age of 40 ± 7 years) due to cardiac failure or cardiac arrest.

Cardiomyopathy was evident in all 18 affected women. Two had hypertrophic cardiomyopathy and five had dilated cardiomyopathy. Permanent pacemakers were placed in three affected women; two subsequently underwent heart transplantation. Myopathy was observed in six women (33%) with mild proximal weakness in proximal limb or neck muscles. Mild mental retardation was noted in one female patient (6%).

Serum creatine kinase was increased in five female patients and ranged from 76 to 643 IU/L. EKG findings were abnormal in all female patients; findings included left ventricular hypertrophy, first-degree atrioventricular block,

sick sinus syndrome, atrial flutter, skipped beat, abnormal Q wave, and complete left bundle branch block.

Family 1 has a frame-shift mutation in exon 9b of the *LAMP-2* gene, which is predicted to affect only the LAMP-2b isoform whereas all other mutations affect both LAMP-2a and 2b isoforms. The two affected members in that family have hypertrophic cardiomyopathy and mild myopathy but no mental retardation. Both female patients are currently alive, ages 23 and 34 years. Two heterozygous women are 56 and 27 years of age and have not developed cardiac abnormalities, muscle weakness, or elevations of serum creatine kinase.

Muscle pathology. Pathologic findings in muscle are summarized in table 3. All probands showed mild to moderate variation in fiber size. Small vacuoles were seen in many fibers, which may appear as basophilic granules rather than vacuoles in hematoxylin and eosin preparations (figure 1). The granules contained acid phosphatase-positive material. In all probands, acetylcholine and nonspecific esterase activities were associated with the vacuolar membranes. Furthermore, on immunohistochemistry the vacuolar membranes stained with antibody against dystrophin, whereas LAMP-2 was completely absent in muscle from all male patients (figure 2).

On electron microscopy, pathologic findings in muscle included numerous intracytoplasmic autophagic vacuoles with glycogen particles and cytoplasmic debris. In addition, some of the vacuoles were bounded by membranes with features of the basal lamina.

Discussion. We identified 13 families, with a total of 20 male and 18 female patients, with genetically confirmed Danon disease. All 13 probands were male, whereas women were less severely affected, with later-onset cardiomyopathy. These findings suggest that Danon disease is an X-linked dominant disorder. In fact, the causative gene for Danon disease, *LAMP-2*, has been mapped to chromosome

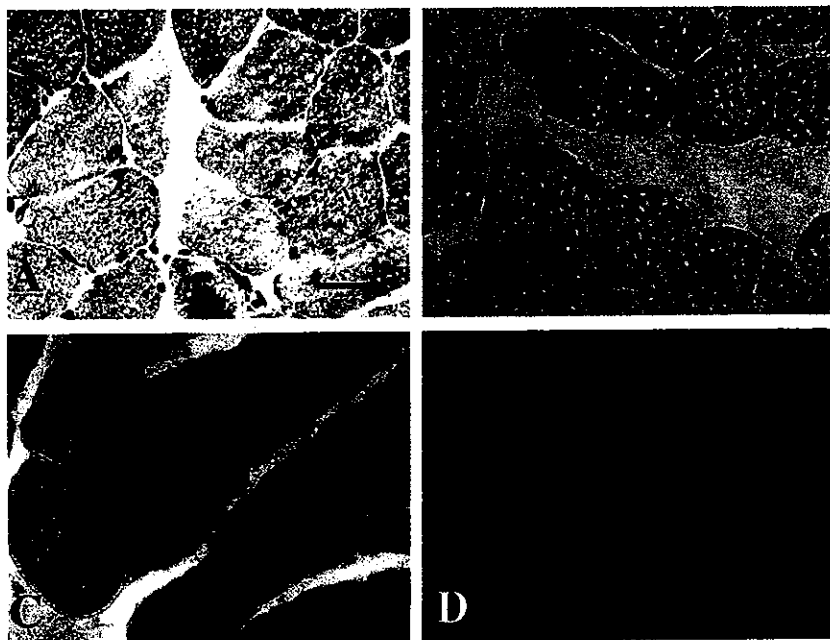


Figure 1. Histochemistry and immunohistochemistry. Transverse sections of skeletal muscle biopsy specimens from affected men with Danon disease. Several fibers with tiny basophilic intracytoplasmic vacuoles are scattered throughout (A). The vacuolar membrane has high acetylcholinesterase (B) and nonspecific esterase (C) activities. Dystrophin expressed in vacuolar membrane and sarcolemma of muscle fibers (D). (A) Hematoxylin and eosin stain. (B) Acetylcholinesterase. (C) Nonspecific esterase. (D) Immunohistochemistry with antibody against dystrophin. Bar = 40 μ m.

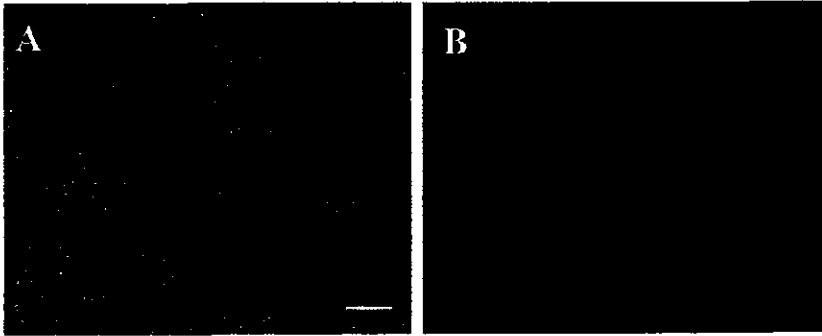


Figure 2. Immunohistochemistry. Transverse sections of skeletal muscle biopsies from control subjects (A) and affected men from Danon disease (B) were immunostained with antibody against LAMP-2. LAMP-2 is present in the control muscles, whereas it is absent in Danon disease muscles. Bar = 40 μ m.

Xq24.³ In previous studies, this disease had been defined clinically by the triad of cardiomyopathy, myopathy, and variable mental retardation. We have confirmed that this clinical triad encompasses the main clinical features of Danon disease.

Myopathy is usually mild and can be clinically silent; however, all male patients had elevated serum creatine kinase levels and myogenic changes by electromyography. Symptomatic patients typically had proximal limb weakness, which was very slowly progressive or stable. Myopathic symptoms were noted in only a few female patients and were even milder. Two female patients without overt myopathy underwent muscle biopsy; one showed no remarkable findings, but the other revealed focal vacuolation in muscle fibers.^{5,11}

Electrophysiologically, in addition to myopathic units in all male patients tested, myotonic discharges were observed in three of 10 male patients; however, clinical myotonia was not evident in any patient. Therefore, myotonic discharges are not uncommon in patients with Danon disease but are observed less frequently than in patients with type II glycogenesis.¹⁷

Cardiac symptoms are the dominant clinical features and the most important prognostic factors, because all of the deceased patients died of cardiac failure. Histologically, cardiomyocytes have shown severe vacuolation and degeneration, including myofibrillar disruption and lipofuscin accumulation.^{5,11}

Most male patients developed hypertrophic cardiomyopathy, whereas most female patients showed dilated cardiomyopathy. Previous reports described the evolution of the hypertrophic into dilated cardiomyopathy with progressive cardiac failure.^{1,7} Therefore, dilated cardiomyopathy may be associated with the timing of cardiac investigation. However, other factors may determine the type of cardiomyopathy.

The WPW EKG pattern observed in Danon disease has been attributed to myocardial hypertrophy rather than to the presence of an accessory pathway.⁶ However, the incidence of WPW is relatively high (6/17 male patients, 35%) in Danon disease as compared with that in other hypertrophic cardiomyopathy, such as idiopathic hypertrophic cardiomyopathy (1.5%) and familial hypertrophic cardiomyopathy (12%),¹⁸ which suggests the presence of a specific pathomechanism for

preexcitation in Danon disease rather than a simple association with cardiac hypertrophy.

Although permanent pacemakers were inserted in several patients, heart transplantation may be the most effective intervention. The only male patient who underwent heart transplantation was a 25-year-old man with hypertrophic cardiomyopathy, atrial flutter, and atrioventricular block. For 4 years after the operation, he did not have significant deteriorations except occasional rejection episodes.¹¹ As in men, cardiomyopathy can be fatal in female patients. This suggests that not only male patients but also women with Danon disease should be considered for heart transplantation. In addition, we suggest that asymptomatic female relatives of male patients should be investigated for cardiomyopathy and followed closely to detect early signs of a potentially life-threatening condition.

Mild mental retardation was observed in more than half of the male patients and electroencephalography showed mild abnormalities in two male patients. One male patient had decreased cerebral glucose metabolism in the cerebral cortex on PET.¹³ There were no CNS manifestations and no patient showed structural brain abnormalities by CT or MRI. However, careful postmortem neuropathologic analysis is needed to further characterize the CNS involvement in Danon disease.

Muscle pathology is characterized by small basophilic vacuoles in many fibers. The vacuolar membranes show acetylcholine and nonspecific esterase activities that are very useful to distinguish Danon disease from other vacuolar myopathies including acid maltase deficiency. The positive acid phosphatase stain is also a useful though not specific diagnostic feature. However, similar vacuoles are also seen in other autophagic vacuolar myopathies including X-linked myopathy with excessive autophagy¹⁹ and infantile autophagic vacuolar myopathy.⁸ The pathognomonic finding in Danon disease is the absence of LAMP-2 immunohistochemical staining.

In *LAMP-2* knockout mice, a wider variety of organs is affected, including liver, kidney, pancreas, small intestine, thymus, and spleen, in addition to heart and skeletal muscle.²⁰ Therefore, other organs may also be involved in Danon disease. In fact, some male patients had hepatomegaly and had dispropor-

tionately high serum aspartate transaminase and alanine aminotransferase levels compared with creatine kinase values. Mild portal fibrosis with normal hepatocytes was seen in liver from one male patient with cardiac dysfunction.¹¹ However, another biopsy specimen from another male patient without cardiopathy showed sclerotic portal and central veins, nuclear vacuolization of the hepatocytes, and enlarged mitochondria with irregular cristae,¹² suggesting that liver may be primarily affected. In addition, there was platelet dysfunction and glycogen accumulation in one other patient.⁹

Human exon 9 of the *LAMP-2* gene exists in two forms, exon 9a and 9b, that are alternatively spliced and produce two isoforms, LAMP-2a and LAMP-2b. LAMP-2a is present ubiquitously, whereas LAMP-2b is expressed predominantly in heart and skeletal muscles.¹⁵ The mutation in Family 1 affects only the LAMP-2b isoform, whereas all other mutations affect both LAMP-2a and 2b isoforms. The two affected men in Family 1 had hypertrophic cardiomyopathy and mild myopathy but no mental retardation. In this family, one affected man is alive at age 34 years and one female patient is alive at age 56 years, suggesting that isolated deficiency of the LAMP-2b isoform may be associated with a milder phenotype.

Most mothers of the probands have shown cardiac abnormalities. This finding is in sharp contrast to the broad range of clinical severity in manifesting carriers of other X-linked recessive disorders, such as Duchenne muscular dystrophy. Although we identified five asymptomatic mothers, all but one (80%) had sporadic affected sons, raising the possibility that these singleton male patients were due to spontaneous mutations. In support of this notion, two of the asymptomatic mothers did not harbor a mutation in blood DNA. All available evidence indicates that Danon disease is an X-linked dominant disease.

Acknowledgment

The authors thank Rika Oketa, Fumie Uematsu, and Saba Tadesse for technical assistance and Dr. Narihiro Minami for his critical advice.

References

- Danon MJ, Oh SJ, DiMauro S, et al. Lysosomal glycogen storage disease with normal acid maltase. *Neurology* 1981; 31:51-57.
- Nishino I, Fu J, Tanji K, et al. Primary LAMP-2 deficiency causes X-linked vacuolar cardiomyopathy and myopathy (Danon disease). *Nature* 2000;406:906-910.
- Mattei MG, Matterson J, Chen JW, Williams MA, Fukuda M. Two human lysosomal membrane glycoproteins, h-lamp-1 and h-lamp-2, are encoded by genes localized to chromosome 13q34 and chromosome Xq24-25, respectively. *J Biol Chem* 1990;265:7548-7551.
- Fukuda M. Biogenesis of the lysosomal membrane. *Subcell Biochem* 1994;22:199-230.
- Byrne E, Dennett X, Crotty B, et al. Dominantly inherited cardioskeletal myopathy with lysosomal glycogen storage and normal acid maltase levels. *Brain* 1986;109:523-536.
- Riggs JE, Schochet SS Jr, Gutmann L, Shanske S, Neal WA, DiMauro S. Lysosomal glycogen storage disease without acid maltase deficiency. *Neurology* 1983;33:873-877.
- Murakami N, Goto YI, Itoh M, et al. Sarcolemmal indentation in cardiomyopathy with mental retardation and vacuolar myopathy. *Neuromuscul Disord* 1995;5:149-155.
- Yamamoto A, Morisawa Y, Verloes A, et al. Infantile autophagic vacuolar myopathy is distinct from Danon disease. *Neurology* 2001;57:903-905.
- Katsumi Y, Tokonami F, Matsui M, Aii H, Nonaka I. A case of glycogen storage disease with normal acid maltase accompanied with the abnormal platelet function. *Rinsho Shinkeigaku* 1994;34:827-831.
- Itoh M, Asano Y, Shimohira M, Iwakawa Y, Goto Y, Nonaka I. A patient with lysosomal glycogen storage disease with normal acid maltase. *No To Hattatsu* 1993;25:459-464.
- Dworzak F, Casazza F, Mora M, et al. Lysosomal glycogen storage with normal acid maltase: a familial study with successful heart transplant. *Neuromuscul Disord* 1994;4:243-247.
- Matsumoto S, Yamada T, Tanaka K, et al. Hepatic involvement in a case of lysosomal glycogen storage disease with normal acid maltase. *Rinsho Shinkeigaku* 1999;39:717-721.
- Katsumi Y, Fukuyama H, Ogawa M, et al. Cerebral oxygen and glucose metabolism in glycogen storage disease with normal acid maltase: case report. *J Neurol Sci* 1996;140:46-52.
- Kawamura H, Shimojo S, Nonaka I, Abe M, Tadokoro M. A case of lysosomal glycogen storage disease with normal acid maltase (Danon) without apparent cardiomyopathy and mental retardation. *Rinsho Shinkeigaku* 2000;40:259-262.
- Konecki DS, Foetisch K, Zimmer KP, Schlotter M, Lichter-Konecki U. An alternatively spliced form of the human lysosome-associated membrane protein-2 gene is expressed in a tissue-specific manner. *Biochem Biophys Res Commun* 1995;215:757-767.
- Takemitsu M, Nonaka I, Sugita H. Dystrophin-related protein in skeletal muscles in neuromuscular disorders: immunohistochemical study. *Acta Neuropathol* 1993;85:256-259.
- Engel AG, Gomez MR, Seybold ME, et al. The spectrum and diagnosis of acid maltase deficiency. *Neurology* 1973;23:95-106.
- Marriott HTL. Electrocardiographic abnormalities, conduction disorders and arrhythmias in primary myocardial disease. *Prog Cardiovasc Dis* 1964;7:99-114.
- Kalimo H, Savontaus M-L, Lang H, et al. X-linked myopathy with excessive autophagy: a new hereditary muscle disease. *Ann Neurol* 1988;23:258-265.
- Tanaka Y, Guhde G, Suter A, et al. Accumulation of autophagic vacuoles and cardiomyopathy in LAMP-2-deficient mice. *Nature* 2000;406:902-906.

Ullrich disease: Collagen VI deficiency: EM suggests a new basis for muscular weakness

Abstract—Ullrich disease is a form of congenital muscular dystrophy characterized clinically by generalized muscle weakness, contractures of the proximal joints, and hyperflexibility of the distal joints from birth or early infancy. Recently, mutations of the collagen VI gene have been associated with Ullrich disease. The authors report on a boy with Ullrich disease who has complete deficiency of collagen VI and harbors compound heterozygous mutations in the collagen VI alpha 2 gene. Absence of microfibrils on EM, together with normal collagen fibrils and basal lamina, suggests that loss of a link between interstitium and basal lamina may be a new molecular pathomechanism of muscular dystrophy.

NEUROLOGY 2002;59:920–923

H. Ishikawa, MD; K. Sugie, MD, PhD; K. Murayama, MD; M. Ito, MD; N. Minami, MS;
I. Nishino, MD, PhD; and I. Nonaka, MD, PhD

In 1930, Ullrich described two boys with an unusual form of congenital muscular dystrophy.¹ The clinical findings included generalized muscle weakness, contractures of the proximal joints, and hyperflexibility of the distal joints from birth or early infancy. He labeled this disorder 'Die kongenitale atonisch-sklerotische Muskeldystrophie.' High-arched palate, protuberant calcanei, and normal intelligence are other characteristics of the disease. Muscle biopsies revealed dystrophic changes.² Recently, two groups found complete deficiency of collagen VI in patients with Ullrich disease.^{3,4} All patients had frameshift type mutations in the gene encoding collagen VI alpha 2 (COL6A2). So far, four different mutations were reported; a single nucleotide insertion at exon 13, a 26-bp deletion in exon 14, an aberrant splicing at the border between intron 17 and exon 18, and exon 24 skipping.

We report a new patient with Ullrich disease and complete deficiency of collagen VI with morphologic abnormalities at the EM level.

Materials and methods. *Patient.* The male patient was the first child of healthy parents who denied consanguinity. At birth, he was noted to have generalized muscle weakness, hypotonia, and contractures of proximal joints. His motor developmental milestones were delayed. He was able to sit unassisted at age 2 years 6 months.

Additional material related to this article can be found on the *Neurology* Web site. Go www.neurology.org and scroll down the Table of Contents for the September 24 issue to find the link for this article.

From the Department of Neuromuscular Research (Drs. Ishikawa, Sugie, Nishino, and Nonaka and N. Minami), National Institute of Neuroscience, National Center of Neurology and Psychiatry (NCNP), Kodaira, Tokyo; Department of Neurology (Dr. Ishikawa), Nihon University School of Medicine, Tokyo; Department of Neurology (Dr. Sugie), Nara Medical University, Nara; Department of Pediatrics (Dr. Murayama), National Rehabilitation Center for Disabled Children, Tokyo; and Department of Pediatrics (Dr. Ito), Metropolitan Bokutoh Hospital, Tokyo, Japan.

Received March 4, 2002. Accepted in final form May 29, 2002.

Address correspondence and reprint requests to Dr. Ichizo Nishino, Department of Neuromuscular Research, National Institute of Neuroscience, National Center of Neurology and Psychiatry (NCNP), 4-1-1 Ogawahigashi-cho, Kodaira, Tokyo 187-8502, Japan; e-mail: nishino@ncnp.go.jp

The patient was diagnosed as having Ullrich disease based on clinical and muscle histology findings at age 3. We examined the patient at the age 4. He could sit but could not walk without assistance (figure 1A). He had generalized muscle weakness and atrophy that was most prominent in the neck. Although facial muscle weakness was equivocal, his palate was clearly high arched. He had severe contractures of the proximal joints, including neck, shoulder, elbow, hip, and knee joints, and had marked kyphoscoliosis. In contrast, distal joints such as hand, ankle, toe, and finger joints were hyperextensible (see figure 1B,C). Other findings included enlarged calcanei (see figure 1C) and diminished or absent tendon jerks. His intelligence was normal. Laboratory examination revealed no specific diagnostic abnormalities. The serum creatine kinase level was slightly elevated (220 to 480 IU/L; normal, 51 to 197 IU/L). Results of a brain CT were normal.

Histochemical and immunohistochemical analyses. Transverse serial frozen muscle sections of 6 μ m or 8 μ m thickness were stained with hematoxylin and eosin, modified Gomori trichrome, and a battery of histochemical techniques. We also immunostained skeletal muscles with the monoclonal antibody against collagen VI (1:500) (ICN Biomedicals, Aurora, OH) and the polyclonal antibody against collagen IV (1:2000) (Advance, Tokyo, Japan).

Sequence analysis of collagen VI alpha 2 gene (COL6A2). Total RNA was extracted from frozen muscle using Totally RNA Kit (Nippon Gene, Tokyo, Japan) and was reverse transcribed into cDNA with oligo (dT)₂₀ primer using the ThermoScript RT-PCR System (Life Technologies, Carlsbad, CA). We amplified two overlapped fragments, encompassing nt 1 to 1330 and nt 1313 to 3147 (nucleotide number is based on AY029208), which cover the entire open reading frame. We directly sequenced the amplified fragments with the PCR primers⁵ and relevant internal primers using BigDye Terminator Cycle Sequencing Kit (PE Biosystems, Foster, CA), and then electrophoresed the samples using an ABI PRISM 377 DNA sequencer (PE Biosystems). RT-PCR using a forward primer in exon 13 (AGG GCC ACA GGT GCT GCC AA) and a reverse primer in exon 15 (GGG CCC GCT TAG CAC CAT GGA) gave at least four bands. Each band was excised and sequenced. To identify the intronic mutations, we amplified the genomic fragments encompassing intron 14 through exon 15 and intron 23 through exon 24. We sequenced the amplified fragments with the PCR primers.³

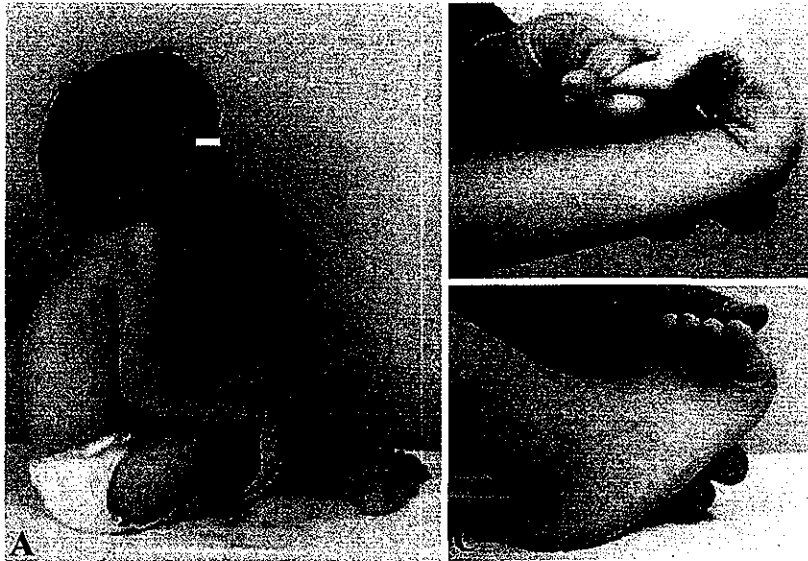


Figure 1. Clinical features of Ullrich disease. (A) The patient is unable to extend his arm due to the contractures of elbow and shoulder joints. Note slender stature with generalized muscle wasting. (B) Hyperextension of the wrist joint. (C) Hyperlaxity of toe joints and protuberant calcanei.

Electron microscopy. Skeletal muscle from the patient was fixed with 2% glutaraldehyde and postfixed in osmium tetroxide, dehydrated in graded alcohol series, and then embedded in Epon (Taab Laboratories Equipment, Ltd., Aldermaston, UK). Ultrathin sections, stained with uranyl acetate and lead citrate, were examined.

Results. Histochemical and immunohistochemical analysis. On histochemical examination, scattered necrotic and regenerating fibers were identified. Moderate endomyssial fibrosis was present (figure 2A). There was type 2 fiber atrophy, and marked type 1 fiber predominance was seen. Fiber type distribution differed from fascicle to fascicle (see figure 2B). On immunohistochemistry, collagen VI was completely absent in the muscle from the patient (see figure 2D), whereas collagen VI was present in sarcolemma and interstitial tissue in normal muscle (see figure 2C) and in other disease control muscle, including Duchenne muscular dystrophy and Fukuyama type muscular dystrophy (data not shown). In contrast, collagen IV, which is a major component of basal lamina, was intact in the patient's muscle (see figure 2F).

Sequence analysis of collagen VI alpha 2 gene (COL6A2). We found compound heterozygous mutations in the COL6A2 gene. One allele had a G-to-C substitution at position -1 in intron 14 (see part B of the supplementary figure, which can be found on the *Neurology* Web site. Go to www.neurology.org and scroll down the Table of Contents for the title link to this article.). Direct sequence of RT-PCR products showed overlapping peaks after exon 14 when read with a forward primer (see part A of supplementary figure on the Web site) and before exon 15 when read with a reverse primer. The sequencing of the shortest band showed that exon 14 was connected to the last 53 bp of intron 14 and exon 15. Likewise, the second shortest band showed that exon 14 was connected to the last 247 bp of intron 14 and exon 15. We were unable to isolate and purify the other bands because they were too close to each other in the gel. The second COL6A2 allele had a C-to-G substitution at position -3 in intron 23 (see part D of

supplementary figure on the Web site.). The direct sequence of the RT-PCR products showed skipping of the entire exon 24. Both mutations were absent in 100 normal chromosomes.

Electron microscopy. The basal lamina was intact even in degenerating muscle fibers (see figure 2G). Collagen fibrils in the interstitium appeared normal, with a periodic pattern of about a 65-nm interval. In contrast, microfibrils, which are usually seen in the interstitium associated with collagen fibrils, were totally absent (see figure 2I).

Discussion. We have identified complete collagen VI deficiency in a patient with Ullrich disease and found compound heterozygous mutations of COL6A2 in the patient. In one allele, a C at -3 position in intron 23 was changed to G. The nucleotide at this position is conserved in only 65% of introns;⁶ however, we did not identify any other polymorphisms in this region. This mutation caused the skipping of the entire exon 24 and is predicted to cause frameshift of the codon, resulting in the elimination of most of the C-terminal globular domain. The same exon 24 skipping was reported in an Italian patient, although the patient had a nucleotide substitution at -1 position in intron 23. The second allele had a G-to-C transition at position -1 in intron 14, causing the insertion of intron 14 of variable size. The inserted fragments that we identified were 53 bp and 247 bp in length; thus, both are predicted to cause a frameshift of the codon, resulting in the elimination of the triple-helical domain and the C-terminal globular domain. RT-PCR analyses revealed abnormal splicing of exons contiguous to the polymorphism, indicating that both are pathogenic mutations.

Collagen VI is thought to be a major protein in microfibrils. The complete absence of microfibrils in our patient with complete collagen VI deficiency suggests this idea. Collagen VI has been shown to anchor the basement membrane in skeletal muscle by

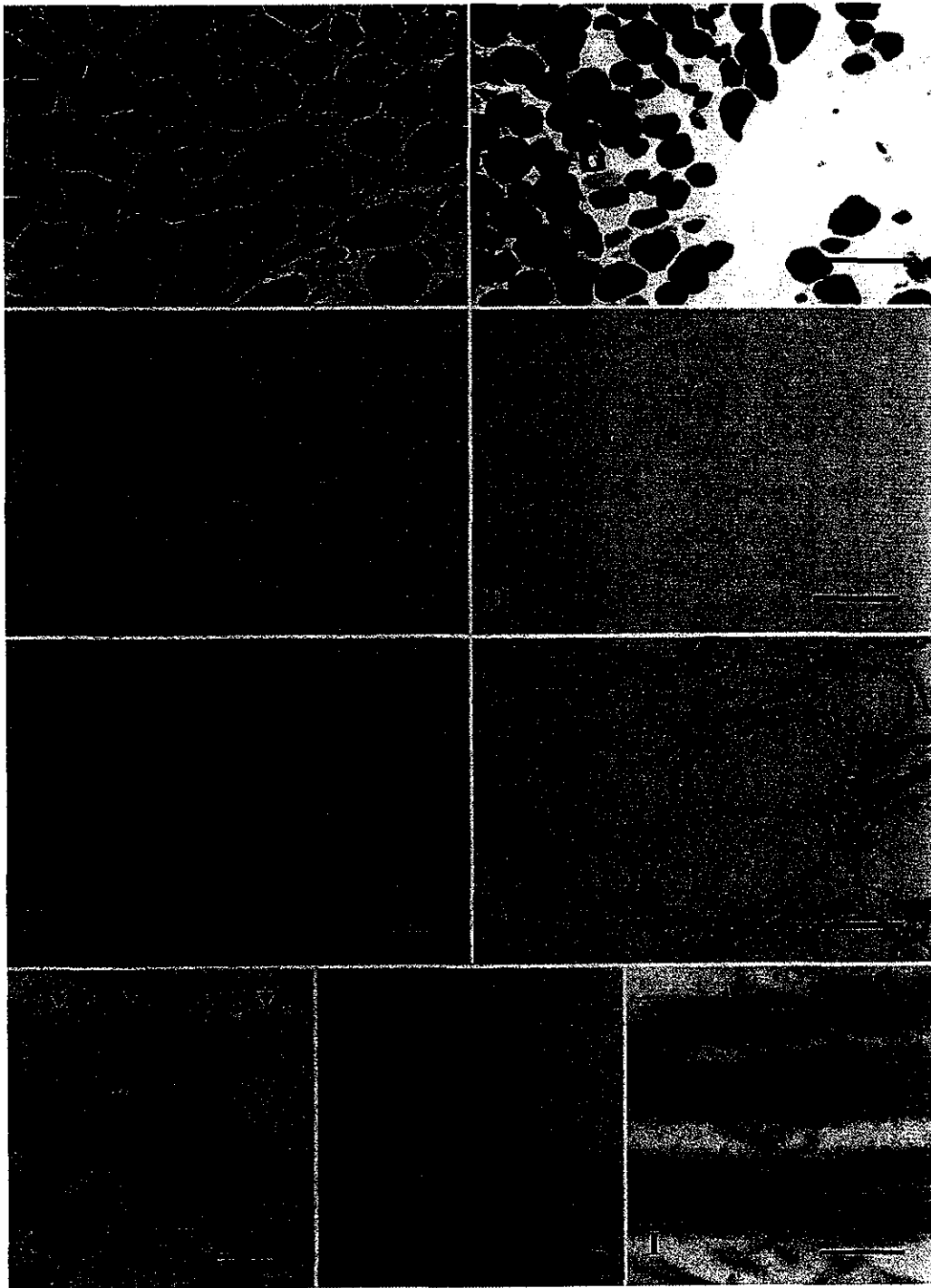


Figure 2. Muscle pathology findings (biceps brachii). (A) Hematoxylin and eosin staining showing necrosis and regeneration with endomysial fibrosis. (B) Histochemical staining for myosin ATPase with preincubation at pH 4.6. Type 1 fiber predominance and scattered type 2C fibers are seen. Fiber-type distribution differs from fascicle to fascicle. (C and D) Immunostaining for collagen VI: normal (C) and the patient's result (D). Collagen VI was completely absent in the patient's muscle. (E and F) Immunostaining for collagen IV: normal (E) and the patient (F). Collagen IV is normally present in sarcolemma in the patient. (G, H, I) Electron micrographs: (G) The basal lamina (arrowheads) is intact even in degenerating muscle fibers. (H) Fukuyama type muscular dystrophy for control. Both collagen fibrils (asterisks), with typical periodic pattern of about 65 nm and about 50 nm in diameter, and microfibrils (arrowheads), with much smaller diameter, are present in the interstitium. (I) In the patient, collagen fibrils (asterisks) are present but microfibrils are totally absent. (Bar = 100 μ m in A and B; 50 μ m in C-F; 1 μ m in G; and 0.5 μ m in H and I.)

interacting with collagen IV, a major component of basal lamina.⁷ Intact basal lamina and collagen fibrils on electron microscopy, together with intact collagen IV expression on immunohistochemical study, suggests that loss of anchoring between the basal lamina and the interstitium may be a new molecular mechanism of congenital muscular dystrophy.

Acknowledgment

The authors thank the patient and his family for their cooperation and vigorous support of this research work; Dr. Michio Hirano for reviewing the manuscript; and Ms. Fumie Uematsu and Ms. Kumiko Murayama for their technical assistance.

References

1. Ullrich O. kongenitale, atonisch-sklerotische Muskeldystrophie, ein weiterer Typus der hereditären Muskelerkrankungen des neuromuskulären Systems. *Z Ges Neurol Psychiat* 1930;126:171-201.
2. Nonaka I, Une Y, Ishihara T, Miyoshino S, Nakashima T, Sugita H. A clinical and histological study of Ullrich's disease (congenital atonic-sclerotic muscular dystrophy). *Neuropediatrics* 1981;12:197-208.
3. Vanegas OC, Bertini E, Zhang RZ, et al. Ullrich scleroatonic muscular dystrophy is caused by recessive mutations in collagen type VI. *Proc Natl Acad Sci USA* 2001;98:7516-7521.
4. Higuchi I, Shiraishi T, Hashiguchi T, et al. Frameshift mutation in the collagen VI gene causes Ullrich's disease. *Ann Neurol* 2001;50:261-265.
5. Pepe G, Bertini E, Giusti B, et al. A novel de novo mutation in the triple helix of the COL6A3 gene in a two-generation Italian family affected by Bethlem myopathy: a diagnostic approach in the mutations' screening of type VI collagen. *Neuromuscul Disord* 1999;9:264-271.
6. Benjamin Lewin. *Genes VII*. Oxford: Oxford University Press, 2000.
7. Kuo EJ, Maslen CL, Keene DR, Glanville RW. Type VI collagen anchors endothelial basement membranes by interacting with type IV collagen. *J Biol Chem* 1997;272:26522-26529.

Novel mutation in X-linked Charcot-Marie-Tooth disease associated with CNS impairment

Abstract—The authors describe a 16-year-old boy with severe muscular atrophy and signs of peripheral neuropathy compatible with Charcot-Marie-Tooth disease. Abnormalities in the cerebellum and central somatosensory pathway were also noted. Gene analysis revealed a novel gross insertion mutation in exon 2 of the connexin32 gene along with a 21-base pair duplication resulting in a seven-amino acid insertion in the first extracellular loop of the protein.

NEUROLOGY 2002;59:923-926

Hideshi Kawakami, MD, PhD; Ken Inoue, MD, PhD; Ichiro Sakakihara; and Shigenobu Nakamura, MD

Charcot-Marie-Tooth disease (CMT) is characterized by distal muscle weakness and amyotrophy, sensory impairment, decreased or absent tendon reflexes, and high arched feet. Autosomal dominant, recessive, and X-linked forms are known.¹ One of the causative genes, which encodes connexin32 (Cx32) in X-linked CMT (CMTX), has been reported.²⁻⁶

Cx32 is a gap junction protein and is found in several tissues, including the liver, secretory epithelium, brain, and peripheral nerves.⁶ In the peripheral nerves, Cx32 is located in the paranodal regions and the Schmidt-Lantermann incisures. In the brain, it is expressed in neurons and oligodendro-

cytes. Although many studies have shown abnormalities in the gene encoding Cx32, the clinical features of CMT seem to differ depending on the type of mutation that has occurred. We report a novel amino acid insertion in the gene encoding Cx32 that resulted in clinical features indicating CNS abnormalities in addition to the classic features of CMT.

Case report. A 16-year-old boy presented with a 6-year history of progressive gait disturbance due to leg muscle weakness. Pes cavus and scoliosis had been noted by his parents at age 8. Disproportionate thinness of the patient's lower legs ("stork legs") was evident a few years before the emergence of a gait disturbance characterized by foot drop and steppage gait. The patient's maternal uncle and a brother of his grandmother had similar findings. Although his parents had no symptoms and unremarkable medical history, his mother showed a prolonged central conduction time in a short latency somatosensory evoked potential (SEP) study (P13-N20 interpeak latency, 7.8 msec; her height, 155 cm; normal average [SD], 6.2 msec [0.4]). Neurologic examinations in the patient revealed normal intelligence. Cranial nerves were intact, but saccadic eye movement for smooth pursuit and slight dysarthria were noted. The results of a manual muscle strength test revealed distal dominant muscle weakness in the extremi-

Additional material related to this article can be found on the *Neurology* Web site. Go to www.neurology.org and scroll down the Table of Contents for the September 24 issue to find the title link for this article.

From the Third Department of Internal Medicine, Hiroshima University School of Medicine, Japan.

Received December 10, 2001. Accepted in final form June 5, 2002.

Address correspondence and reprint request to Dr. Hideshi Kawakami, Third Department of Internal Medicine, Hiroshima University School of Medicine, Kasumi 1-2-3 Minami-ku Hiroshima, 734-8551 Japan; e-mail: hkawakam@hiroshima-u.ac.jp

Distal myopathy with rimmed vacuoles is allelic to hereditary inclusion body myopathy

I. Nishino, MD, PhD; S. Noguchi, PhD; K. Murayama, BS; A. Driss, PhD; K. Sugie, MD, PhD; Y. Oya, MD; T. Nagata, MD, PhD; K. Chida, MD, PhD; T. Takahashi, MD, PhD; Y. Takusa, MD; T. Ohi, MD, PhD; J. Nishimiya, MD, PhD; N. Sunohara, MD, PhD; E. Ciafaloni, MD; M. Kawai, MD, PhD; M. Aoki, MD, PhD; and I. Nonaka, MD, PhD

Abstract—Background: Distal myopathy with rimmed vacuoles (DMRV) is an autosomal-recessive disorder with preferential involvement of the tibialis anterior muscle that starts in young adulthood and spares quadriceps muscles. The disease locus has been mapped to chromosome 9p1-q1, the same region as the hereditary inclusion body myopathy (HIBM) locus. HIBM was originally described as rimmed vacuole myopathy sparing the quadriceps; therefore, the two diseases have been suspected to be allelic. Recently, HIBM was shown to be associated with the mutations in the gene encoding the bifunctional enzyme, UDP-*N*-acetylglucosamine 2-epimerase/*N*-acetylmannosamine kinase (*GNE*). **Objective:** To determine whether DMRV and HIBM are allelic. **Methods:** The *GNE* gene was sequenced in 34 patients with DMRV. The epimerase activity in lymphocytes from eight DMRV patients was also measured. **Results:** The authors identified 27 unrelated DMRV patients with homozygous or compound-heterozygous mutations in the *GNE* gene. DMRV patients had markedly decreased epimerase activity. **Conclusions:** DMRV is allelic to HIBM. Various mutations are associated with DMRV in Japan. The loss-of-function mutations in the *GNE* gene appear to cause DMRV/HIBM.

NEUROLOGY 2002;59:1689–1693

Distal myopathy with rimmed vacuoles (DMRV), originally described in 1981, is an autosomal-recessive disorder characterized clinically by the preferential involvement of the tibialis anterior muscle with sparing of quadriceps muscles.^{1–3} The age at onset ranges from 15 to 40 years, with an average of 26 years. The initial symptom is usually altered gait. Patients become wheelchair-bound between 26 and 57 years of age, on average 12 years after the onset of symptoms. Muscle biopsy is characterized by many rimmed vacuoles, especially in atrophic fibers. Necrotic and regenerating fibers are rarely seen. The rimmed vacuoles occasionally contain congophilic amyloid material and deposits that are immunoreactive to β -amyloid and β -amyloid precursor proteins, ubiquitin and tau protein. The nucleus occasionally contains tubulofilamentous inclusions of 15 to 20 nm in diameter.^{2,3}

Hereditary inclusion body myopathy (HIBM), which was originally described in 1983 as “rimmed vacuole

myopathy” sparing the quadriceps, is an autosomal-recessive disorder very similar to DMRV both clinically and pathologically.^{3,4} Both diseases were mapped to the same region on chromosome 9, naturally raising the question of whether the two diseases are allelic.^{5,6} Recently, HIBM was shown to be associated with mutations in the gene encoding a bifunctional enzyme, UDP-*N*-acetylglucosamine 2-epimerase/*N*-acetylmannosamine kinase (*GNE*).⁷ To determine whether DMRV is genetically identical to HIBM, we screened 34 unrelated patients with DMRV for mutations in the *GNE* gene.

Patients and methods. All patients were Japanese, except for Patient 3, who is a North American of German and Irish origin. Patients were diagnosed as having DMRV based on both clinical features and muscle pathology. All the patients were unrelated. We also studied DNA from the parents of Patients 2, 3, 4, and 22, the mother of Patient 5, and six unaffected family members of Patient 8. We extracted genomic DNA from frozen muscle or lym-

See also pages 1674, 1776, and 1808

From the Department of Neuromuscular Research (Drs. Nishino, Noguchi, Driss, and Sugie and M. Murayama), National Institute of Neuroscience, National Center of Neurology and Psychiatry (NCNP), Kodaira, Tokyo; the Department of Neurology (Drs. Oya and Kawai), National Center Hospital for Mental, Nervous, and Muscular Disorders (Dr. Nonaka), NCNP; the Department of Neurology (Dr. Nishimiya), Kohnodai Hospital, NCNP, Kohnodai, Chiba; the Department of Neurology (Drs. Nagata and Chida), Iwate National Hospital, Iwate; the Department of Neurology (Dr. Takahashi), Nishitaga National Hospital, Sendai; the Department of Pediatrics (Dr. Takusa), Shimane Medical University, Shimane; Division of Neurology (Dr. Ohi), Department of Internal Medicine, Miyazaki Medical College, Miyazaki; Sunohara Medical Clinic (Dr. Sunohara), Kawasaki, Japan; Duke University Medical Center (Dr. Ciafaloni), Durham, NC; and Department of Neurology (Dr. Aoki), Tohoku University School of Medicine, Sendai, Japan

Received May 20, 2002. Accepted in final form September 28, 2002.

Address correspondence to Dr. Ichizo Nishino, Department of Neuromuscular Research, National Institute of Neuroscience, National Center of Neurology and Psychiatry (NCNP), 4-1-1 Ogawahigashi-cho, Kodaira, Tokyo, 187-8502 Japan; e-mail: nishino@ncnp.go.jp

Copyright © 2002 by AAN Enterprises, Inc. 1689

Copyright © Lippincott Williams & Wilkins. Unauthorized reproduction of this article is prohibited.

phocytes using a phenol chloroform method. We amplified each exon and flanking sequences of the *GNE* gene by PCR and the directly sequenced the amplified fragments. We used the same primer sets with those used for screening HIBM.⁷

To ascertain the frequency of the three common *GNE* mutations, 578A>T, 1765C>C, and 1939G>A, among Japanese, we screened DNA of 50 control individuals. We used mismatch primer-based restriction fragment length polymorphism (RFLP) for 578A>T and 1765G>C. For 578A>T, a new *Mae* III site was introduced to mutant DNA only by amplifying the fragments with exon 3 forward primer (E3F) and CTGATATCCATGTGTGAGGAC-CACG (mismatch nucleotide is italicized). For the 1765G>C mutation, a new *Mbo* I site was introduced to only mutant DNA by amplifying the fragments with E10F and TGCTGCAGAACTGGGCCACCTTGAT. For G1939A, we amplified a 344-bp fragment with E11F and E11R and digested the PCR product with *Alu* I since 1939G>A eliminates one of four *Alu* I recognition sites in the fragment. To determine the effect of a possible splice-site mutation in intron 4, we amplified the muscle cDNA from the patient with primers covering the whole open reading frame and with primers covering the region from exon 4 to exon 12. We also amplified the fragment encompassing the exon 3 to 6. We also directly sequenced these fragments.

We performed genetic linkage studies using an ABI 310 Genetic Analyzer and GeneScan program (Applied Biosystems, Foster City, CA) for Patient 8 and his six unaffected family members including parents, sibling, and three father's siblings and compared their haplotypes to Patient 19. The 5'FAM-labeled microsatellite markers used are D9S1804, D9S1794, D9S1209, D9S1791, and D9S1874. Marker order was determined using the public database.

To gain insight into the molecular pathomechanism of DMRV, we assayed UDP-GlcNAc 2-epimerase activity in leukocytes from eight DMRV patients (table) and from 13 controls.⁸ Peripheral leukocytes were homogenized in 200 mM MES (pH 7.2) containing 0.15 M NaCl, 10mM CaCl₂, 1% Triton X-100, 4mg/mL aprotinin, 1mM phenylmethylsulfonylfluoride, 0.2 mM uridine, 0.5 mM ManNAc, 1mM dithiothreitol by brief sonication and centrifuged at 20,000 g for 30 minutes at 4 °C. From each supernatant, an aliquot containing 200 to 500 µg of protein was incubated with 1 µCi of ³H-UDP-GlcNAc in a total volume of 0.08 mL. After incubation for 30 minutes at 37°C, the reaction was terminated by boiling. The produced *N*-acetylhexosamine was separated from substrate by amine-adsorption HPLC, and its radioactivity was measured. Since the activity of UDP-GlcNAc 2-epimerase is inhibited by CMP-NeuNAc,⁹ we measured the amount of hexosamine both with and without 100 µM CMP-NeuAc and used this difference to determine the activity of UDP-GlcNAc 2-epimerase.

Results. We identified homozygous or compound-heterozygous mutations in 27 patients (see the table and figure 1). We identified 12 different mutations: 10 missense, a 10-bp insertion, and one intron mutation. Among them, three mutations, 1765G>C, 578A>T, and 1939G>A, were shared by more than one patient. These three common mutations were absent in 100 control chromosomes from normal Japanese individuals, indicating that they are not common polymorphisms among Japanese people.

The adenine nucleotide at +4 position in the intron is

conserved (68%),¹⁰ raising the possibility that the intron 4 mutation in Patient 5 causes exon 4 skipping. Even in normal controls exon 4 skipping occurs at low levels (figure 2). In Patient 5, however, exon 4 skipping is abundant. Furthermore, the mutation in the other allele, 1765G>C, was heterozygous when the fragment covering the whole open reading frame was directly sequenced, but it appeared to be homozygous when the fragment amplified with a forward primer that annealed to exon 4. This result indicates that the intronic mutation drives the frequency of a normally occurring rare illegitimate splicing event to almost 100%, resulting in virtually complete exon 4 skipping mutation in the allele.

The mutations cosegregated with the disease in all families except in the family of Patient 8. We found a homozygous 578A>T mutation in a healthy father of Patient 8, who was 60 years of age and did not have any muscle weakness. Patient 19 also has a homozygous 578A>T mutation. Haplotype analysis using markers flanking the *GNE* gene showed that Patient 19's haplotypes are completely distinct from those of Patient 8's father. We confirmed that one of the alleles in Patient 8 was transmitted from his father. These results indicate that in these two families, the homozygous 578A>T mutation has arisen in different genetic backgrounds and some other factor may be modulating expression of this mutation. The mother of Patient 5 had a heterozygous 1043T>C gene mutation.

The epimerase activity in DMRV patients (0.97 fmol/mg protein/minute ± 1.64) (mean ± SD) was significantly reduced as compared with that in controls (14.7 ± 12.3; *p* < 0.005; figure 3). The epimerase activity of Patient 8's unaffected father, who has a homozygous 578A>T mutation, has been determined twice: 5.29 and 2.47 fmol/mg protein/minute.

Discussion. DMRV and HIBM have been suspected of being the same disease because both clinical and pathologic features of the two diseases are quite similar and because both diseases were mapped to the same region on chromosome 9. We found homozygous or compound heterozygous mutations in the *GNE* gene in patients with DMRV. Together with a recently reported Japanese DMRV patient with compound heterozygous *GNE* gene mutations, 1765>C and 1430C>T,¹¹ our data indicate that DMRV is allelic to HIBM. Moreover, as in HIBM,⁷ most of the DMRV-associated mutations were missense, although the sites of the mutations are different and homozygous null mutations were not identified. The 1765G>C mutation accounts for 61% (33/54) of the abnormal alleles in our series, indicating a high frequency of carriers of this mutation in Japan, although none of control alleles had it. We are currently haplotyping patients with the 1765 mutation. Our preliminary data suggest that the high frequency of the 1765 mutation is due to a founder effect. A similar result has also been reported by another group.¹² The exon 4 skipping mutation identified in Patient 5 is in-frame because the exon 4 consists of 153 nucleotides. The only null mutation was the 10-bp insertion in Patient 27, albeit heterozygous, which causes a frame-shift of the codon.

Table Identified mutations

Patient	Mutation	Exon/intron	Predicted amino acid alteration	Protein domain
1	580C>T	E3	R177C	Epimerase
	1765G>C	E10	V572L	Kinase
2*	1765G>C	E10	V572L	Kinase
	1765G>C	E10	V572L	Kinase
3	1183>T	E7	D378Y	Kinase
	1943C>T	E11	A631V	Kinase
4*	1765G>C	E10	V572L	Kinase
	1765G>C	E10	V572L	Kinase
5	IVS4+4A>G	I4	Exon 4 skipping	Epimerase
	1765G>C	E10	V572L	Kinase
6	1765G>C	E10	V572L	Kinase
	1765G>C	E10	V572L	Kinase
7	1765G>C	E10	V572L	Kinase
	1765G>C	E10	V572L	Kinase
8*	578A>T	E3	D176V	Epimerase
	1043T>C	E6	V331A	Kinase
9*	1765G>C	E10	V572L	Kinase
	1765G>C	E10	V572L	Kinase
10	447C>G	E3	H132Q	Epimerase
	578A>T	E3	D176V	Epimerase
11	1765G>C	E10	V572L	Kinase
	1765G>C	E10	V572L	Kinase
12*	578A>T	E3	D176V	Epimerase
	1765G>C	E10	V572L	Kinase
13	1765G>C	E10	V572L	Kinase
	1765G>C	E10	V572L	Kinase
14	1765G>C	E10	V572L	Kinase
	1765G>C	E10	V572L	Kinase
15	1765G>C	E10	V572L	Kinase
	1765G>C	E10	V572L	Kinase
16	578A>T	E3	D176V	Epimerase
	1939G>A	E11	A630T	Kinase
17*	578A>T	E3	D176V	Epimerase
	1939G>A	E11	A630T	Kinase
18*	578A>T	E3	D176V	Epimerase
	1466T>C	E9	I472T	Kinase
19*	578A>T	E3	D176V	Epimerase
	578A>T	E3	D176V	Epimerase
20	1765G>C	E10	V572L	Kinase
	1765G>C	E10	V572L	Kinase
21	1765G>C	E10	V572L	Kinase
	1765G>C	E10	V572L	Kinase
22	578A>T	E3	D176V	Epimerase
	968G>A	E5	R306Q	Epimerase
23	1765G>C	E10	V572L	Kinase
	1765G>C	E10	V572L	Kinase
24	1765G>C	E10	V572L	Kinase
	1765G>C	E10	V572L	Kinase
25	1765G>C	E10	V572L	Kinase
	1765G>C	E10	V572L	Kinase
26	578A>T	E3	D176V	Epimerase
	1765G>C	E10	V572L	Kinase
27	10 bp insertion	E2	Frame shift	Epimerase
	1765G>C	E10	V572L	Kinase

* Patients whose lymphocytes were examined for enzymatic assay for the epimerase activity.

E = exon; I = intron.

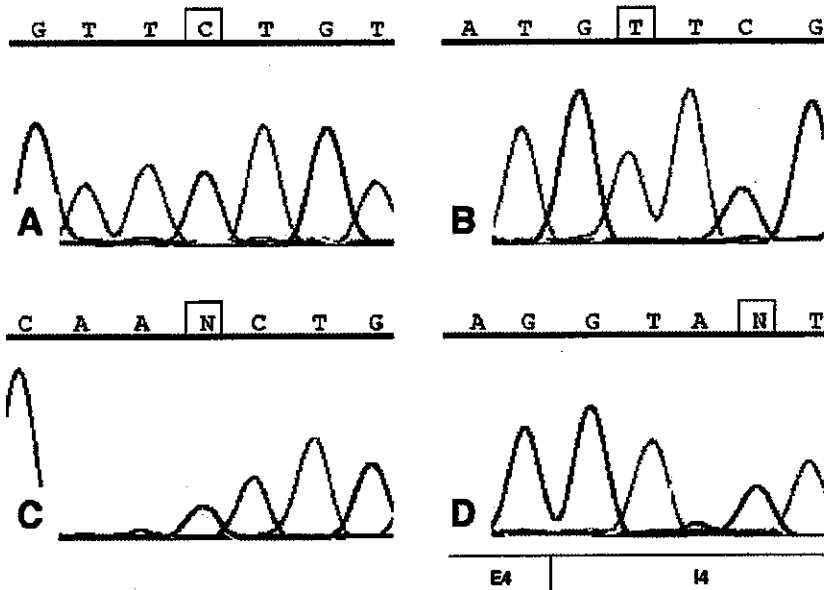


Figure 1. Electropherogram of representative *GNE* gene mutations. (A) Homozygous 1765G>C mutation in Patient 2. (B) Homozygous 578A>T mutation in Patient 19. (C) Heterozygous 1939G>A mutation in Patient 17. (D) Splice-site mutation in Patient 5. Heterozygous A to G mutation is present at the fourth nucleotide in intron 4.

In our series, we also found compound heterozygous mutations in a North American patient with DMRV who is of German and Irish origin (Patient 3). This result indicates that DMRV is not restricted in Japan.

The high frequency of missense mutations together with absence of homozygous null mutations in DMRV and in HIBM raises the possibility that total loss-of-function might be lethal or even that the loss of enzymatic function of *GNE* might not be the mechanism responsible for the development of the disease. However, we showed that the epimerase activity of *GNE* is significantly decreased in lymphocytes from the patients with DMRV, suggesting that the loss-of-function mutations in the *GNE* gene are likely to be the cause of the disease. In five patients, the epimerase activity was below the detectable level

in our study. This may imply that some of the mutations are functionally equivalent to null mutations. More likely, however, the absence of detectable activity is because the normal range of activity is low in lymphocytes as compared to other organs such as liver. The wide range of the epimerase activity in nor-

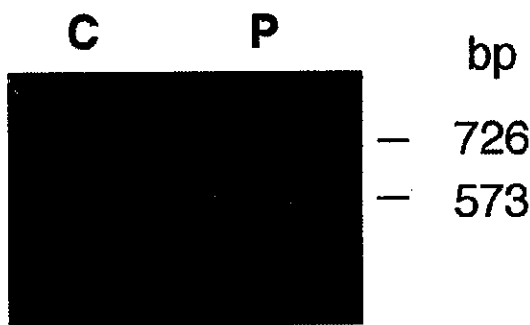


Figure 2. Exon 4 skipping in Patient 5. Muscle cDNA was amplified with the primers in exon 3 and 6 that normally yield a 726-bp fragment. A shorter fragment (573 bp) was seen in Patient 5 (P). The difference (153 bp) is exactly the same with the size of exon 4. We also sequenced the fragment and confirmed the exon 4 skipping. A faint band of the same size can also be seen in a control (C), suggesting that aberrant splicing occurs even in normal individuals, albeit in small amounts.

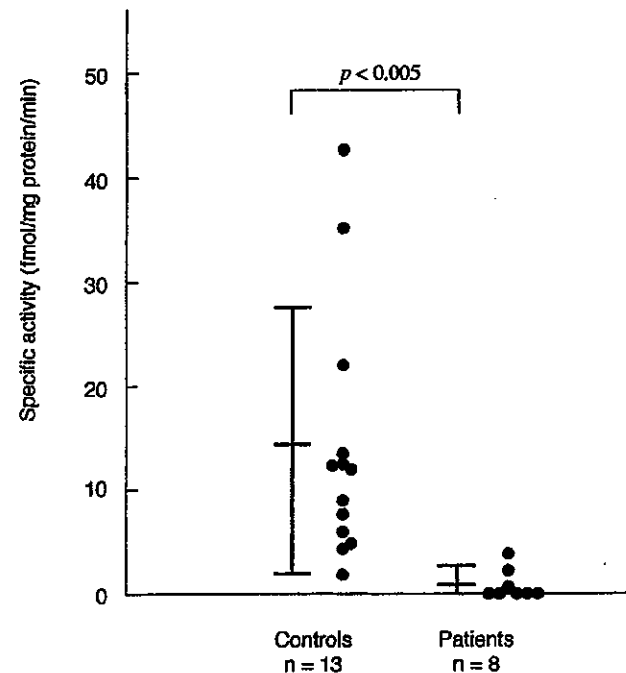


Figure 3. Biochemical assay for the UDP-N-acetylglucosamine 2-epimerase activity in leukocytes from DMRV patients. The epimerase activity in DMRV patients ($0.97 \text{ fmol/mg protein/minute} \pm 1.64$) (mean \pm SD) were significantly reduced as compared with that in controls (14.7 ± 12.3 ; $p < 0.005$). Patients examined are noted with an asterisk in the table.

mal controls may also be due to technical difficulties related to measuring low activities in lymphocytes.

It has been shown that either epimerase or kinase activity can be lost selectively by site-directed mutagenesis while retaining the activity of the counterpart, suggesting that the two active sites function independently.¹³ But this is probably not the case in vivo since lymphocytes from all eight patients had low epimerase activity, including three homozygous mutations in the kinase domain (see figure 3). Furthermore, we found four patients with compound-heterozygous mutations in the epimerase and kinase domains, indicating that complementation between the two domains is not operating in these patients.

The identification of a healthy individual with a homozygous *GNE* gene mutation suggests the incomplete penetrance of the disease. In fact, incomplete penetrance has also been suspected in a healthy 67-year-old person of Persian Jewish origin who carries the common M712T *GNE* gene mutation in a homozygous form (Drs. Argov and Mitrani-Rosenbaum, personal communication). Alternatively, the father may have another mutation that rescues the 578A>T mutation in a noncoding region that we did not sequence. Another possibility is that 578A>T mutation is a neutral polymorphism. However, this is unlikely because of the rather high frequency of the mutation and the absence of the mutation in controls. The epimerase activity of Patient 8's father is in the low-normal range. Because our range of normal enzyme activity is wide and overlaps with the patients' range, we need to develop a more sensitive and specific biochemical assay for future studies.

The identification of seven patients without mutations in the *GNE* gene and no clinicopathological differences compared to patients with mutations may be due to unidentified mutations in the noncoding sequence or promoter region, or these patients may have a genetically distinct disease. Further studies are necessary to address this issue.

Acknowledgment

The authors thank all the patients and their family members for their cooperation; Drs. H. Ishikawa and A. Yamamoto for their technical support; Drs. M. Imazawa, T. Tsukahara, Y.K. Hayashi, N. Minami, T. Toda, and H. Sugita for their critical comments; and Dr. M. Hirano for reviewing the manuscript.

References

1. Nonaka I, Sunohara N, Ishiura S, Satoyoshi E. Familial distal myopathy with rimmed vacuole and lamellar (myeloid) body formation. *J Neurol Sci* 1981;51:141-155.
2. Nonaka I, Murakami N, Suzuki Y, Kawai M. Distal myopathy with rimmed vacuoles. *Neuromuscul Disord* 1998;8:333-337.
3. Nonaka I. Distal myopathies. *Curr Opin Neurol* 1999;12:493-499.
4. Argov Z, Yarom R. 'Rimmed vacuole myopathy' sparing the quadriceps: a unique disorder in Iranian Jews. *J Neurol Sci* 1984;64:33-43.
5. Mitrani-Rosenbaum S, Argov Z, Blumenfeld A, Seidman CE, Seidman JG. Hereditary inclusion body myopathy maps to chromosome 9p1-q1. *Hum Mol Genet* 1996;5:159-163.
6. Ikeuchi T, Asaka T, Saito M, et al. Gene locus for autosomal recessive distal myopathy with rimmed vacuoles maps to chromosome 9. *Ann Neurol* 1997;41:432-437.
7. Eisenberg I, Avidan N, Potikha T, et al. The UDP-N-acetylglucosamine 2-epimerase/N-acetylmannosamine kinase gene is mutated in recessive hereditary inclusion body myopathy. *Nat Genet* 2001;29:83-87.
8. Seppala R, Tietze F, Kransnewich D, et al. Sialic acid metabolism in sialuria fibroblasts. *J Biol Chem* 1991;266:7456-7461.
9. Seppala R, Lehto V-P, Gahl WA. Mutations in the human UDP-N-acetylglucosamine 2-epimerase gene define the disease sialuria and the allosteric site of the enzyme. *Am J Hum Genet* 1999;64:1563-1569.
10. Lewin B. *Genes VII*, New York: Oxford University Press, 2000.
11. Kayashima T, Matsuo H, Satoh A, et al. Nonaka myopathy is caused by mutations in the UDP-N-acetylglucosamine-2-epimerase/N-acetylmannosamine kinase gene (*GNE*). *J Hum Genet* 2002;47:77-79.
12. Arai A, Ikeuchi T, Igarashi S, et al. Search for a causative gene for distal myopathy with rimmed vacuoles [in Japanese]. Presented at the 43rd Annual Meeting of the Japanese Neurological Society, May 30, 2002; Sapporo, Japan.
13. Effertz K, Hinderlich S, Reuter W. Selective loss of either the epimerase or kinase activity of UDP-N-acetylglucosamine 2-epimerase/N-acetylmannosamine kinase due to site-directed mutagenesis based on sequence alignments. *J Biol Chem* 1999;274:28771-28778.

Mutation in the caveolin-3 gene causes a peculiar form of distal myopathy

Abstract—The authors describe a patient with sporadic distal myopathy associated with reduced caveolin-3 in muscle fibers in which the muscle atrophy was restricted to the small muscles of the hands and feet. Gene analysis disclosed a heterozygous 80 G→A substitution in the caveolin-3 gene that was identical to that of reported cases of elevated serum creatine kinase. This patient further demonstrated possible clinical heterogeneity of myopathies with mutations in the caveolin-3 gene.

NEUROLOGY 2002;58:323–325

M. Tateyama, MD; M. Aoki, MD; I. Nishino, MD; Y.K. Hayashi, MD; S. Sekiguchi, MD; Y. Shiga, MD; T. Takahashi, MD; Y. Onodera, BSc; K. Haginoya, MD; K. Kobayashi, MD; K. Inuma, MD; I. Nonaka, MD; K. Arahata, MD; and Y. Itoyama, MD

Caveolin-3 is the muscle-specific protein product of the caveolin gene family and a principal integral membrane component of caveolae.¹ Caveolin may function as a scaffolding protein for organizing and concentrating caveolin-interacting molecules and may play a pivotal role in essential cellular functions such as signal transduction and lipid metabolism.²

Recently, mutations in the human caveolin-3 gene have been shown to cause autosomal-dominant limb girdle muscular dystrophy.³ Subsequently, other mutations in the caveolin-3 gene have been reported to be associated with sporadic cases in infants with elevated serum creatine kinase.^{4,5} These findings imply that caveolin-3 gene mutations may cause various forms of myopathies.

We report a sporadic case of a patient with a peculiar form of distal myopathy in which the caveolin-3 gene mutation was identical to that in cases of infants with elevated serum creatine kinase, reported previously.⁴

Case report. The patient was first admitted to the pediatric division of our hospital at the age of 12 because of palpitation. Her serum creatine kinase concentration was 2,092 IU/L (normal, <135). Slight atrophy was suspected only in her hypothenar muscles. Needle electromyography showed myopathic changes restricted to the distal parts of the upper extremities such as the opponens pollicis. A biopsy specimen from the biceps brachii revealed mild myopathic changes. Although infrequent premature contractions were observed, cardiac functions were normal. She did not have difficulties in her daily life during junior high school or high school. When she was admitted to

another hospital at age 25 because of gastritis, elevated serum creatine kinase was noticed again by a physician. She was then referred to our hospital. Her parents were unrelated, and the family history was negative for neuromuscular disorders. Serum levels of creatine kinase in her parents were normal.

On examination, her height was 170 cm and her weight was 70 kg. Her musculature was well developed and muscle atrophy was observed only in the small muscles of her hands and feet (figure 1). The muscle strength of the proximal limbs, forearms, and trunk were normal, except for mild weakness in neck flexion. She could stand on the tips of her toes and heels. The grasping power was 23 kg in the right hand and 26 kg in the left hand. In both hands, the muscle strength was moderately reduced in the palmar interossei and opponens pollicis muscles, and slightly reduced in the dorsal interossei muscles. Deep tendon reflexes were normally elicited. All sensory perception tests were normal. Her serum creatine kinase concentration was 2,154 IU/L, aspartate aminotransferase concentration was 57 IU/L (normal, <35), and lactate dehydrogenase activity was 816 IU/L (normal, <453). The serum level of total cholesterol was slightly elevated at 267 mg/dL (normal, <220 mg/dL). Chest roentgenogram and electrocardiogram showed no abnormalities.

Needle electromyography showed myopathic motor unit potentials of decreased duration and amplitude on volition in the first dorsal interossei, deltoid, and sternocleidomastoid muscles. No spontaneous activities were observed in any of the muscles examined. Motor and sensory nerve conduction studies were normal in both upper and lower limbs. The muscle biopsy specimen from the biceps brachii showed a mild variation in fiber size, increased centrally placed nuclei, and type 1 fiber predominance.

Methods. *Immunohistochemistry and Western blot analysis.* Frozen muscle sections were prepared from the patient and from normal control tissue. Antibodies used for immunohistochemistry included monoclonal antibodies against caveolin-3 (BD Transduction laboratories, Lexington, KY), dystrophin, β -dystroglycan, merosin, and polyclonal antibodies against α -sarcoglycan and dysferlin, which was described previously.⁶ Western blot analysis was performed using the monoclonal antibody for caveolin-3 and the polyclonal antibody for dysferlin. The muscle samples were processed as described previously.⁶

Genetic analysis. Genomic DNA extracted from peripheral blood lymphocytes of the patient, after informed

From the Departments of Neurology (Drs. Tateyama, Aoki, Sekiguchi, Shiga, Takahashi, Onodera, and Itoyama) and Pediatrics (Drs. Haginoya and Inuma), Tohoku University School of Medicine, Sendai; Departments of Ultrastructural Research (Drs. Nishino and Nonaka) and Neuromuscular Research (Drs. Nishino, Hayashi, and Arahata), National Center of Neurology and Psychiatry (NCNP), Tokyo; and Department of Neurology (Dr. Kobayashi), Yamagata City Hospital Saiseikan, Japan.

Supported by grants-in-aid from the Japan Foundation for Aging and Health, and the Ministry of Health, Labor and Welfare (M.A., I.N., Y.K.H., I.N., K.A.) and grants-in-aid for Scientific Research (B, 12557058) from the Japan Society for Promotion of Science (M.A., Y.I.).

Received July 6, 2001. Accepted in final form October 7, 2001.

Address correspondence and reprint requests to Dr. Maki Tateyama, Department of Neurology, Tohoku University School of Medicine, 1-1 Seiryomachi, Aoba-ku Sendai 980-8574, Japan; e-mail: mtateyama@neuro.med.tohoku.ac.jp

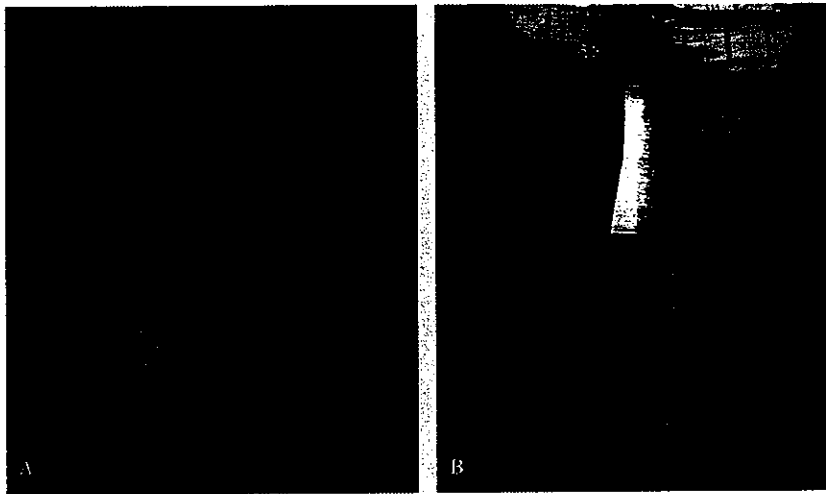


Figure 1. (A) The right hand of the patient shows muscle atrophy in the thenar and hypothenar muscles. (B) The feet of the patient show muscle atrophy on both sides of each foot. In contrast, the calf muscles and anterior tibial muscles are well developed.

consent, was used as a template for PCR amplification.³ Direct sequence analysis of PCR products for the caveolin-3 gene was performed using an ABI 377 Sequencer (PE Applied Biosystems, Foster City, CA). The 80 G→A mutation identified in this way was confirmed by analysis of genomic DNA by restriction enzyme digestion with *Bsa*I as described.⁴

Results. By immunohistochemical examinations, dystrophin, α -sarcoglycan, β -dystroglycan, and merosin were normally expressed on muscle fibers. However, the immunoreaction of caveolin-3 and dysferlin was markedly reduced compared with the control (figure 2). Results of Western blot analysis of dysferlin were normal both in size and amount, whereas caveolin-3 was almost absent (data not shown). Sequence analysis of the caveolin-3 gene revealed a G→A substitution on one allele at position 80 causing an amino acid change of an arginine for a glutamine at position 27 (figure 3). We confirmed the mutation with enzyme digestion of PCR products. We did not detect this mutation in 50 normal Japanese control subjects.

Discussion. Mutations in the caveolin-3 gene were first reported in autosomal-dominant limb girdle muscular dystrophy in which the major clinical features were calf hypertrophy and mild to moderate proximal weakness.³ Two other mutations were re-

portedly associated with sporadic cases of elevated serum creatine kinase in infants. One of them had a 136 G→A substitution that also caused myalgia and cramps in the lower limbs, without muscle weakness.⁵ The other had an 80 G→A substitution that caused asymptomatic elevated serum creatine kinase.⁴ The mutation of the caveolin-3 gene in the current case was also an 80 G→A substitution, but the clinical features were different from any cases previously reported.

The term "distal myopathy" is commonly used when distal parts of the limbs are predominantly affected from the early stage of the disease in myopathies. Usually, forearm and leg muscles are affected in addition to hand and foot muscles. For example, in Welander's type distal myopathy, wrist extensor muscles are commonly involved.⁷ The tibialis anterior muscles are involved in distal myopathy with rimmed vacuoles, and the gastrocnemius muscles are invariably involved in Miyoshi myopathy.^{8,9} In contrast, in the current case, beside slight neck weakness, the muscle atrophy was restricted to the small muscles of the hands and feet. This finding may suggest neurogenic atrophy, but we could not find evidence of neurogenic atrophy using electrophysiologic examinations and biopsy. Because needle electromyography in the hand muscles showed myopathic

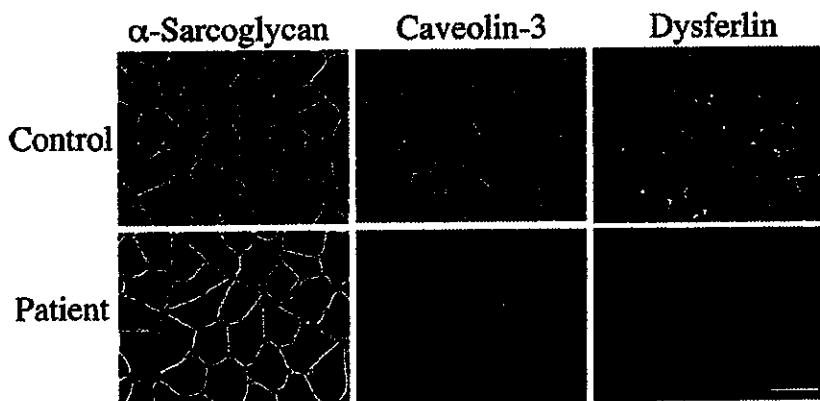


Figure 2. Immunofluorescent staining of skeletal muscles. Normal expression of α -sarcoglycan but reduced expressions of caveolin-3 and dysferlin at the sarcolemma are observed in the patient compared with control. Bar = 100 μ m.

Direct Sequence of caveolin 3 gene

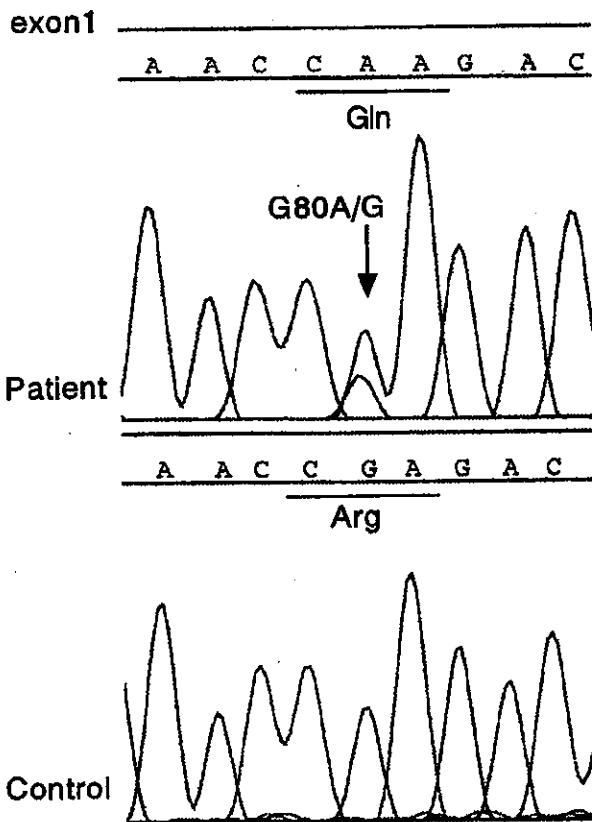


Figure 3. Direct sequence analysis of the caveolin-3 gene. The heterozygous G→A mutation at nucleotide 80 is observed with an amino acid change of the arginine 27 for glutamine (upper panel, arrow). This change is absent in normal controls (lower panel).

motor unit potentials until 12 years of age, we concluded that her muscle atrophy in the small muscles of the hands and feet was caused by myogenic atrophy from the beginning. We think that our patient has unique clinical features distinct from the known types of distal myopathies.

By immunohistochemistry, not only the sarcolemmal expression of caveolin-3 but also that of dysferlin was reduced in the patient. Because results of Western blot analysis of dysferlin were normal, dysferlin expression at the sarcolemma might be second-

arily decreased, as reported in sarcoglycanopathies and dystrophinopathies.¹⁰ Our results indicate that caveolin-3 deficiency should also be considered in patients with reduced sarcolemmal expression of dysferlin.

The current case strongly suggests that mutation of the caveolin-3 gene may cause not only myopathies with proximal weakness but also myopathies with distal weakness. This is analogous to cases with mutations in the dysferlin gene that can cause both proximal (limb girdle muscular dystrophy type 2B) and distal muscular dystrophy (Miyoshi myopathy).⁹ The distinctions among these clinical phenotypes require the identification of additional factors, such as modifier genes that might reveal the mechanism for muscle involvement.⁹ A detailed understanding of the pathogenesis by this mutation in the caveolin-3 gene should highlight the factors that lead to the selective pattern of muscle involvement in muscular dystrophy.

Acknowledgment

The authors thank Mr. Brent Bell for reading this manuscript.

References

1. Song KS, Scherer PE, Tang Z, et al. Expression of caveolin-3 in skeletal, cardiac, and smooth muscle cells. *J Biol Chem* 1996;271:15160–15165.
2. Murata M, Peränen J, Schreiner R, Wieland F, Kurzchalia TV, Simons K. VIP21/caveolin is a cholesterol-binding protein. *Proc Natl Acad Sci USA* 1995;92:10339–10343.
3. Minetti C, Sotgia F, Bruno C, et al. Mutations in the caveolin-3 gene cause autosomal dominant limb-girdle muscular dystrophy. *Nat Genet* 1998;18:365–368.
4. Carbone I, Bruno C, Sotgia F, et al. Mutation in the CAV3 gene causes partial caveolin-3 deficiency and hyperCKemia. *Neurology* 2000;54:1373–1376.
5. Herrmann R, Straub V, Blank M, et al. Dissociation of the dystroglycan complex in caveolin-3-deficient limb girdle muscular dystrophy. *Hum Mol Genet* 2000;9:2335–2340.
6. Matsuda C, Aoki M, Hayashi YK, Ho MF, Arahata K, Brown RH Jr. Dysferlin is a surface membrane-associated protein that is absent in Miyoshi myopathy. *Neurology* 1999;53:1119–1122.
7. Welander L. Myopathia distalis tarda hereditaria. *Acta Med Scand* 1951;141(suppl 265):1–124.
8. Nonaka I, Sunohara N, Ishiura S, Satoyoshi E. Familial distal myopathy with rimmed vacuole and lamellar (myeloid) body formation. *J Neurol Sci* 1981;51:141–155.
9. Liu J, Aoki M, Illa I, et al. Dysferlin, a novel skeletal muscle gene, is mutated in Miyoshi myopathy and limb girdle muscular dystrophy. *Nat Genet* 1998;20:31–36.
10. Piccolo F, Moore SA, Ford GC, Campbell KP. Intracellular accumulation and reduced sarcolemmal expression of dysferlin in limb-girdle muscular dystrophies. *Ann Neurol* 2000;48:902–912.

should this ever be an acceptable strategy for any infected individual?

Finally, we can no longer delay the adoption of an international standard of care for all individuals living with HIV-1, regardless of their reproductive status and where they live. Marginalised populations, including the homeless and the displaced urban and rural poor, are quite capable of adhering to effective HIV therapies. Adherence rates in several African settings surpass those of the developed world.¹⁵ Last week the world witnessed the official opening (sanctioned by the World Trade Organisation) of the first fissure in international trade barriers to the global distribution of inexpensive generic antituberculosis, anti-malaria, and antiretroviral agents.¹⁶ Generic antiretrovirals, prepared in convenient single-pill triple combinations for once and twice daily dosing, are now available for less than US\$1 a day. The HIVNET 012 protocol was modified in 1998 to accommodate the changing realities of the HIV-1 pandemic. 5 years later, these realities have shifted yet again. Suboptimum single-agent and double-agent prophylaxis protocols no longer have a justifiable place in the front lines of the global struggle against HIV/AIDS. It is up to all of us to focus on development of equitable distribution and effective use of these agents now. Once they are widely available, it may be too late.

I have no conflict of interest to declare.

Karen Palmore Beckerman

Bellevue Hospital Center, New York University School of Medicine,
NY 10016, USA
(e-mail: Karen.Beckerman@msnyuhealth.org)

- Guay LA, Musoke P, Fleming T, et al. Intrapartum and neonatal single-dose nevirapine compared with zidovudine for prevention of mother-to-child transmission of HIV-1 in Kampala, Uganda: HIVNET 012 randomised trial. *Lancet* 1999; 354: 795-802.
- Shaffer N, Chuachoowong R, Mock PA, et al. Short-course zidovudine for perinatal HIV-1 transmission in Bangkok, Thailand: a randomised controlled trial. *Lancet* 1999; 353: 773-80.
- The Petra Study Team. The Petra trial: the efficacy of three short-course regimens of zidovudine and lamivudine (3TC) in preventing early and late transmission of HIV-1 from mother to child in an African setting: a randomised, double-blind placebo-controlled trial, conducted in South Africa, Tanzania, and Uganda. *Lancet* 2002; 359: 1178-86.
- Eshleman SH, Mraona M, Guay LA, et al. Selection and fading of resistance mutations in women and infants receiving nevirapine to prevent HIV-1 vertical transmission (HIVNET 012). *AIDS* 2001; 15: 1951-57.
- Kantor R, Lee E, Johnston E, et al. Rapid flux in non-nucleoside reverse transcriptase inhibitor resistance mutations among subtype C HIV-1 infected women after single dose nevirapine. 2nd IAS Conference on HIV Pathogenesis and Treatment, Paris, France, July 13-16, 2003: abstr 78.
- Nduati R, John G, Mbori-Ngacha D, et al. Effect of breastfeeding and formula feeding on transmission of HIV-1: a randomized clinical trial. *JAMA* 2000; 283: 1167-74.
- Nakiyingi JS, Bracher M, Whitworth JA, et al. Child survival in relation to mother's HIV infection and survival: evidence from a Ugandan cohort study. *AIDS* 2003; 17: 1827-34.
- Bloland P, Slutsker L, Steketee RW, Wirima JJ, Heymann DL, Breman JG. Rates and risk factors for mortality during the first two years of life in rural Malawi. *Am J Trop Med Hyg* 1996; 55: 82-86.
- Mullman School of Public Health, Columbia University. MTCT Plus: expanding HIV/AIDS care in resource-limited settings. <http://www.mtctplus.org/www.mtctplus.org> (accessed Sept 7, 2003).
- Havlik DV, Eastman S, Gamst A, Richman DD. Nevirapine-resistant human immunodeficiency virus: kinetics of replication and estimated prevalence in untreated patients. *J Virol* 1996; 70: 7894-99.
- Mandlebrot L, Landreau-Mascaro A, Rekacewicz C, Berrebi A. Lamivudine-zidovudine combination for prevention of maternal-infant transmission of HIV-1. *JAMA* 2001; 285: 2083-93.
- Hernankova M, Ray SC, Ruff C, et al. HIV-1 drug resistance profiles in children and adults with viral load of <50 copies/ml receiving combination therapy. *JAMA* 2001; 286: 196-207.
- Antinori A, Zaccarelli M, Cingolani A, et al. Cross-resistance among nonnucleoside reverse transcriptase inhibitors limits recycling efavirenz after nevirapine failure. *AIDS Res Hum Retroviruses* 2002; 18: 835-38.
- Center for Disease Control and Prevention. Public Health Service task force recommendations for the use of antiretroviral drugs in pregnant HIV-infected women for maternal health and interventions to reduce perinatal HIV-1 transmission in the United States. 2003: <http://www.aidsinfo.nih.gov/guidelines> (accessed Sept 8, 2003).
- McNeil DG. Africans outdo Americans in following AIDS therapy. *New York Times* Sept 3, 2003.
- Becker E. Poor nations can purchase cheap drugs under accord. *New York Times* Aug 31, 2003.

Membrane-repair machinery and muscular dystrophy

Disruption of the plasma membrane is a common event in various normal animal cells, and membrane-repair machinery is essential to prevent disruption-induced cell death. In skeletal muscle, membrane disruptions are most often observed under physiological conditions, because muscle fibres contract repeatedly and are often susceptible to varying degrees of mechanical stress. The fragility of the sarcolemma makes it unable to withstand the mechanical stress, and a defective membrane-repair easily results in necrosis of the muscle fibres.

Muscular dystrophy is characterised by progressive muscle weakness and wasting, with necrosis and regeneration of muscle fibres. Since dystrophin was identified as the gene product responsible for Duchenne muscular dystrophy (the most common form of muscular dystrophy) in 1987, several muscular dystrophies have been associated with instability of the sarcolemma.¹ Lack of a component of the dystrophin-glycoprotein complex (DGC) at the sarcolemma results in instability of the entire complex and thus disrupts the structural linkage between the subsarcolemmal cytoskeleton and the extracellular matrix. Dysferlin is a sarcolemmal protein, and its deficiency causes proximal and distal forms of recessively inherited muscular dystrophies, designated as limb-girdle muscular dystrophy type 2B, Miyoshi's myopathy, and anterior compartment myopathy. Because dysferlin is a homologue of a nematode gene that mediates vesicle fusion to the plasma membrane in spermatids, it has been suggested that dysferlin is involved in membrane fusion.

Recently, Dimple Bansal and colleagues² investigated dysfunction in the membrane-repair machinery in muscular dystrophy. They produced dysferlin-null mice that had muscular dystrophy with a structurally stable sarcolemma and no change in the expression of DGC components. They showed that dysferlin accumulated at sites of membrane disruption in normal muscle (figure), although other sarcolemmal proteins, including caveolin-3 and δ -sarcoglycan, were lost at the site of injury. When they directly assessed resealing efficiency, laser-damaged membrane of wild-type mouse muscle resealed within a minute in the presence of Ca^{2+} ; this Ca^{2+} -dependent resealing of injured sarcolemma was defective in dysferlin-null muscle fibres. These results suggest a direct role of dysferlin in the Ca^{2+} -dependent membrane-repair process.

Non-necrotic muscle fibres from dysferlin-deficient patients early on show membrane abnormalities, including small defects in the plasma membrane, replacement of the plasma membrane by one to multiple layers of small vesicles, and small subsarcolemmal vacuoles.³ These findings are similar to those observed by Bansal and colleagues in dysferlin-null mouse muscle, which have accumulations of vesicles beneath the disrupted cell membrane. For rapid repair of the disrupted membrane, vesicles must accumulate and fuse with the plasma membrane. Abnormal accumulation of subsarcolemmal vesicles in dysferlin-deficient muscles indicates a defective membrane-fusion process.

Osteopontin Plays an Important Role in the Development of Medial Thickening and Neointimal Formation

Kikuo Isoda, Kenichirou Nishikawa, Yashuhiro Kamezawa, Mikoto Yoshida, Masatoshi Kusuhara, Masao Moroi, Norihiro Tada, Fumitaka Ohsuzu

Abstract—Osteopontin (OPN) is a soluble secreted phosphoprotein that binds with high affinity to several integrins and it has been found at the site of atherosclerotic lesions. However, the role of OPN expression in vivo is still poorly understood. To investigate the physiological role of OPN in detail, we generated transgenic mice (Tg) overexpressing the OPN gene under control of the cytomegalovirus enhancer/chicken β -actin promoter. We detected OPN mRNAs in almost all tissues of 3 lines of Tg mice by Northern blotting. The serum levels of OPN were significantly higher in Tg than in non-Tg mice (782 ± 107 versus 182 ± 44 ng/mL; $P < 0.001$). Compared with non-Tg mice, a 73% (88 ± 6 versus 51 ± 7 μ m; $P < 0.001$) and 94% (126 ± 15 versus 73 ± 11 μ m; $P < 0.0001$) increase in the medial thickness of the aorta was determined in Tg mice at 16 and 32 weeks after birth. However, we found no evidence of inflammatory cells adhering to endothelial cells, intimal hyperplasia, or calcification in any region of Tg mice without artery injury. We then investigated the effect of cuff-induced injury to the femoral artery. The intimal thickening in Tg mice increased 2.9-fold more than that in non-Tg mice (4.9 ± 1.9 versus 1.7 ± 0.4 μ m; $P = 0.022$). The expression of OPN induces both medial thickening without injury and neointimal formation after injury, thus suggesting that OPN plays a role in the development of atherosclerosis, vascular remodeling, and restenosis after angioplasty in vivo. (*Circ Res.* 2002;91:77-82.)

Key Words: aorta ■ atherosclerosis ■ genes ■ inflammation ■ smooth muscle

Osteopontin (OPN) is a phosphoprotein that was originally isolated from the bone. It possesses the tripeptide sequence Arg-Gly-Asp like other extracellular matrix proteins and serum proteins such as fibronectin, vitronectin, and collagen.^{1,2} OPN functions as a cell adhesion and migration molecule that can bind to several ligands including $\alpha_v\beta_3$ integrin, CD44, and fibronectin.³⁻⁵ A wide range of cell types including some epithelia, macrophages, T cells, and vascular smooth muscle cells (SMCs) express OPN in a constitutive or inducible fashion.⁶⁻⁹ OPN has recently emerged as a key factor in both vascular remodeling and in the development of atherosclerosis.¹⁰⁻¹² In vitro studies have shown that OPN also promotes the proliferation of cultured rat vascular SMCs¹³ and human coronary artery SMCs.¹⁴ Furthermore, a previous study has shown OPN to stimulate Arg-Gly-Asp-dependent endothelial migration in vitro.¹⁵ However, the function of OPN in the vessel walls is still not yet well understood. The present study uses OPN transgenic mice (Tg) to determine the effect of OPN on SMCs in vivo and to investigate the effect of cuff-induced injury to the femoral artery in vivo. Our results show that OPN overexpression is associated with a significant increase in medial thickening

with aging in vivo and in intimal thickening after arterial injury.

Materials and Methods

Construction of Transgene

We prepared a transgene construct containing the cytomegalovirus enhancer/chicken β -actin (CAG) promoter with cDNA to murine OPN. The CAG-OPN transgene was constructed by inserting the 1.35-kb *EcoRI* fragment containing mouse OPN cDNA sequence into the *EcoRI* site of the third exon of the rabbit β -globin gene in pBsCAG-2.^{16,17} OPN cDNA contains 34 bp of the 5' noncoding region, 885 bp of the coding region, and 429 bp of the 3' untranslated region. Sequencing revealed that the OPN cDNA was identical to the described mouse OPN cDNA.¹⁸ The resulting plasmid was termed pCAG/OPN-9. The CAG-OPN transgene was isolated from the pCAG/OPN-9 backbone by *SalI* and *BamHI* digestion.

Generation and Identification of Transgenic Mice

Transgenic animals were generated by microinjecting purified CAG-OPN construct into the pronuclei of hybrid eggs from B6C3F1 \times C57BL/6 strain parents (Charles River Japan). The tails of the offspring were biopsied at 3 weeks of age. Genomic DNA was isolated using proteinase K. Transgenic mice were identified by Southern blotting. Genomic DNA (10 μ g) was digested with *EcoRI*, which released the 1.35-kb internal fragment of the CAG-OPN

Original received February 18, 2002; revision received May 2, 2002; accepted May 28, 2002.
From First Department of Internal Medicine (K.I., K.N., Y.K., M.Y., M.K., F.O.), National Defense Medical College, Saitama; Third Department of Internal Medicine (M.M.), Toho University School of Medicine, Ohashi Hospital; and the Division of Biomedical Research Resources, Juntendo University School of Medicine (N.T.), Bunkyo-ku, Tokyo, Japan.
Correspondence to Kikuo Isoda, MD, PhD, The First Department of Internal Medicine, National Defense Medical College, 3-2, Namiki, Tokorozawa, Saitama, 359-8513, Japan. E-mail isoda@me.ndmc.ac.jp
© 2002 American Heart Association, Inc.

Circulation Research is available at <http://www.circresaha.org>

DOI: 10.1161/01.RES.0000025268.10302.0C

construct. All blotted membranes were probed with 1.35-kb mouse OPN cDNA labeled with [³²P] dCTP using a random prime labeling kit (Boehringer Mannheim). The National Defense Medical College Board for Studies in Experimental Animals approved the studies.

Northern Blot Analysis

Fifteen micrograms of RNAs were subjected to electrophoresis and then were transferred to a nylon membrane. The RNAs were fixed on this membrane. Hybridization was performed as described previously.¹⁹

Femoral Artery Injury

The animals were anesthetized with an intraperitoneal injection of pentobarbital (50 mg/kg). The left femoral artery was exposed under sterile conditions, and a nonocclusive, flexible polyethylene cuff (length 2 mm; internal diameter 0.56 mm; Becton Dickinson) was placed around the femoral artery to induce intimal thickening, as described.²⁰ The right femoral artery was dissected from the surrounding tissues (sham-operated), but no cuff was put in place. The skin was closed with a series of sutures. The mice were killed 14 days after cuff placement for a morphometric analysis.

Tissue Preparation and Histology

After tail-cuff, systolic blood pressure was measured in the mice, then the animals were euthanized with pentobarbital and perfused with 0.9% NaCl followed by 10% formalin through a 22-gauge angiocatheter placed in the left ventricle of the heart. The aorta and femoral artery were fixed in 10% formalin for 48 hours and embedded in paraffin. Serial 10- μ m sections cut from the aorta or femoral artery were examined by staining with hematoxylin-eosin and Masson's trichrome, as well as by immunohistochemistry.

Morphometry

We examined the hematoxylin-eosin-stained tissue specimens by morphometry. The thickness of the intima and media were measured in each aorta from uninjured mice. Regarding the morphometric analyses of the femoral artery, 10 cross-sections from the cuffed left femoral artery and the control right femoral artery were photographed for each animal. For each artery section, the thickness of the intima and media were measured. Regarding the area/volume calculations, 4 measurements were made using an image analysis computer program (NIH Image; National Institutes of Health): luminal circumference, luminal area, area inside the inner elastic lamina, and area inside the outer elastic lamina. The mean vascular diameter was calculated as luminal circumference/ π . The intima was defined as the area between the lumen and the internal elastic lamina. The media was defined as the area between the internal and external elastic laminae. The volumes of the intima and media were calculated by integrating the areas over the length of the cuffed region.²⁰ The observers of the sections were blinded to the genotype of the mice. The intraassay variability, using independent observers or analyzing adjacent sections from the same vessel, was <3.

Immunohistochemistry and Enzyme

Immunoassay (EIA)

Immunohistochemistry was proceeded on paraffin-embedded sections. The following primary antibodies were used: a rat anti-mouse IgG antibody raised against OPN (Immuno-Biological Laboratory), a primary rat monoclonal antibody against mouse macrophage, clone MOMA-2 (BioSource International), and polyclonal rabbit anti-mouse proliferation cell nuclear antigen (PCNA) antibody (Santa Cruz Biotechnology). The sections were visualized using a Vectastain ABC kit (Vector Laboratories, Inc) with diaminobenzidine (DAB) as the substrate. The plasma OPN concentration was measured using an EIA kit (Immuno-Biological Laboratory).

Substrate Gel Zymography

The protein extracts of aortic tissue were prepared as previously reported,²¹ and samples (10 μ g) were resolved by nonreducing 10%

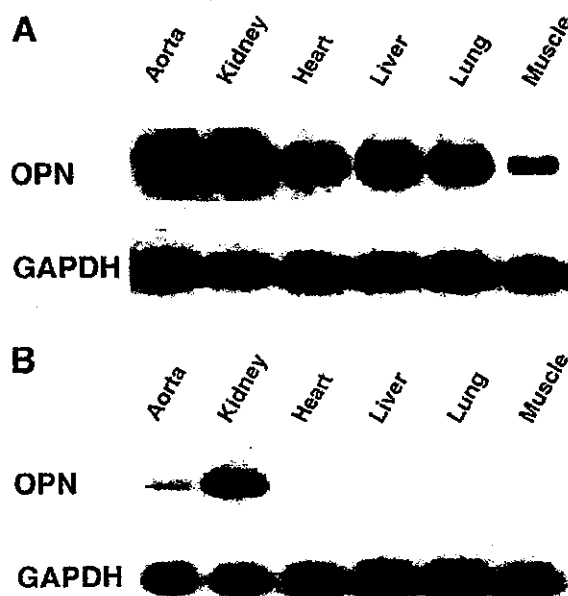


Figure 1. OPN mRNA expression in various tissues from OPN-Tg (A) and non-Tg (B) mice. Northern blots of 15 μ g total RNA from each tissue were hybridized with a ³²P-labeled 1.35-kb mouse OPN probe. GAPDH served as an inner marker. Signal intensity of each gene was normalized for GAPDH.

SDS-PAGE through gels containing 1 mg/mL gelatin. The gels were washed with 2.5% Triton X-100 to remove the SDS, and then were incubated overnight at 37°C in 50 mmol/L Tris-HCl, pH 8.5, 5 mmol/L CaCl₂, and 0.5 mmol/L ZnCl₂. The zones of lysis were visualized after staining the gels with 0.5% Coomassie blue R-250. A densitometric analysis was performed using the NIH Image.

Aortic SMC Explant Migration

The descending aorta was thoroughly dissected free from connective tissue, cut open longitudinally, and the intima and a thin portion of the subjacent media were removed. The descending aorta was weighed and trimmed to normalize the weight to 10 mg. The aorta was cut into 4 pieces and each piece was placed into a separate well of a 6-well plate containing DMEM+20% FBS.

Statistical Analysis

The results are shown as the mean \pm standard deviation. Two groups were compared using Student's *t* test or Student-Newman Keuls's test with the 1-way analysis of variance. A value of *P*<0.05 was regarded as a significant difference.

Results

Generation of Transgenic Mice

We obtained 7 lines of Tg, and 3 lines of them showed high expression of OPN. We examined the expression of OPN mRNA in 6-week-old homozygous Tg mice and in non-Tg mice. These 3 lines expressed high levels of OPN mRNA in almost all tissue specimens, and the kidney and aorta expressed OPN mRNA in both Tg and non-Tg mice (Figures 1A and 1B). The serum levels of OPN determined by EIA were significantly higher in OPN-Tg than in non-Tg mice (Tg, 782 \pm 107 ng/mL [*n*=6]; non-Tg, 182 \pm 44 ng/mL [*n*=6], 6 weeks old; *P*<0.0001). Homozygous Tg mice showed poor growth, osteopenia, and a higher death rate than the non-Tg mice. Despite an absence of death in non-Tg mice at 12

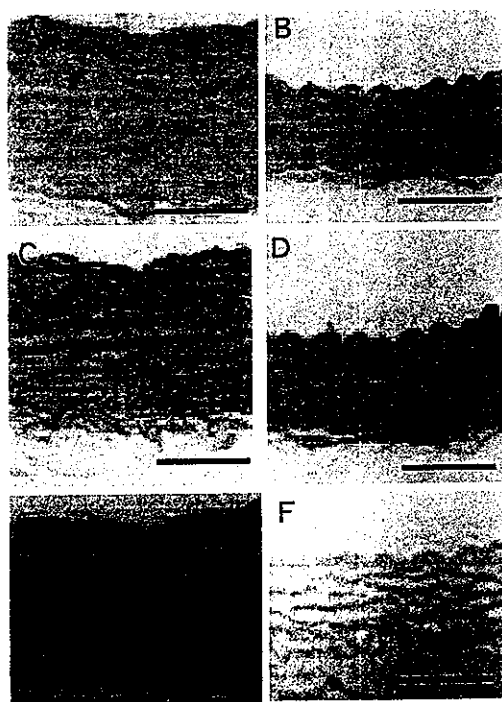


Figure 2. Histology and immunochemical staining of OPN-Tg (left) and non-Tg (right) mouse aortas harvested 32 weeks after birth. Sections were adjacent sections processed for hematoxylin and eosin staining (A and B), elastin staining (C and D), and immunohistochemical staining for OPN (E and F). Bar=50 μ m.

months, the cumulative mortality rate of Tg mice at the same time was 43% (35 of 81 Tg mice were found to have died spontaneously). The dead Tg mice showed a high rate of malignant tumors in liver and/or intestine and/or lung (data not shown). Because homozygous Tg mice were infertile, we crossbred heterozygous male and heterozygous female mice to obtain homozygous offspring. Regarding blood pressure, systolic blood pressure of OPN-Tg mice was as low as that of non-Tg mice (OPN-Tg [n=10, 32 weeks old], 108 \pm 12 mm Hg versus non-Tg [n=10, 32-week-old], 101 \pm 12 mm Hg; *P*=NS). Male and female mice did not differ markedly.

Histology of Aorta

We characterized the changes mainly in the vessel. Figure 2 shows the ascending aorta of OPN-Tg and non-Tg mice 32 weeks after birth that were fed with normal chow. Hematoxylin and eosin staining (Figures 2A and 2B) revealed an increase in the medial thickness and the number of nuclei of SMCs, but no evidence of inflammatory cells adhering to endothelial cells, intimal hyperplasia, or calcification in any region in the OPN-Tg mice. Furthermore, no macrophages (staining for MOMA-2) were detected in either OPN-Tg or non-Tg mice (data not shown). Masson's trichrome-stained sections (Figures 2C and 2D) showed the destruction of the elastic lamina in OPN-Tg. Figures 2E and 2F showed that the medial layers of the aorta derived from OPN-Tg mice were positive for the anti-mouse OPN antibody, whereas the aorta from the non-Tg mice was negative despite little expression

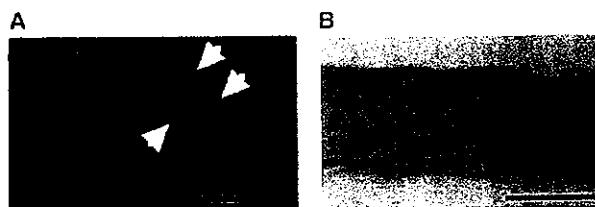


Figure 3. Immunochemical staining for PCNA of OPN-Tg (A) and non-Tg (B) mouse aorta harvested 6 weeks after birth. Mayer's hematoxylin counterstaining is shown. Arrowheads indicate positive nuclei. Bar=20 μ m.

of OPN mRNA. Moreover, OPN was essentially detected in the SMCs of the media of OPN-Tg mice. We next performed PCNA staining to find any evidence of cell proliferation in the SMCs of the media of OPN-Tg mice. The nuclei of SMCs of OPN-Tg mice stained positively for PCNA (Figure 3A). In contrast, the nucleus of non-Tg mice did not stain for PCNA (Figure 3B). These results indicated that the increased medial thickness in OPN-Tg is actually due to an increased proliferation of SMCs.

We next investigated the change of medial thickness dependent on aging (Figure 4). At 6 weeks old, the medial thickness of the aorta in the OPN-Tg tended to be larger (but not significant) than that of non-Tg mice (OPN-Tg [n=10], 41 \pm 4 μ m; non-Tg [n=10], 36 \pm 4 μ m, NS). At 16 weeks old, the medial thickness of the aorta in the OPN-Tg mice increased by 73% (88 \pm 6 μ m, n=10) in comparison to the non-Tg mice (51 \pm 7 μ m, n=10; *P*<0.001). At 32 weeks old, the medial thickness in OPN-Tg mice increased by 94% (126 \pm 15 μ m, n=10) compared with non-Tg mice (73 \pm 11 μ m, n=10; *P*<0.0001). These findings indicated the period between adolescence and young adulthood (between 6 weeks and 16 weeks old) to be the time when the biggest increase in the medial thickness occurs (from 14% to 73%) and that this increase in the medial thickness in OPN-Tg may be related to body development.

Intimal Thickening After Injury

We investigated the effect of cuff-induced injury to the femoral arteries of OPN-Tg mice at 16 weeks old. Figure 5

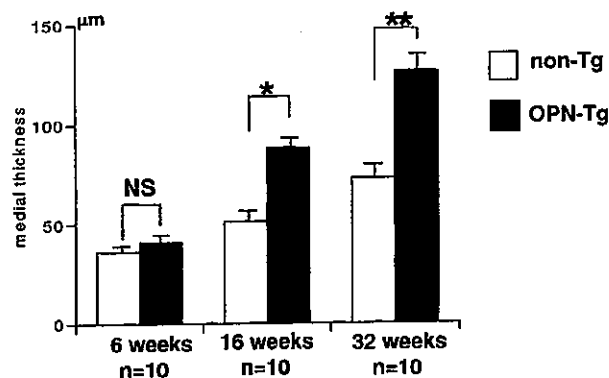


Figure 4. Comparison of the medial thickness of the ascending aorta between 6- (left), 16- (middle), and 32- (right) week-old OPN-Tg and non-Tg mice. Values represent the mean \pm SD. NS indicates not significant. **P*<0.001; ***P*<0.0001.